



ORIGINAL COPY
REC'D 9/10/07
R.P. Know
PLANNING.

Condition Appraisal and Structural Review
Miami Marine Stadium Roof Structure
Miami, Florida

Volume I - Report

prepared for

The Hartford Steam Boiler
Inspection and Insurance Co.
One State Street
Hartford, Connecticut 06102

02174

02174

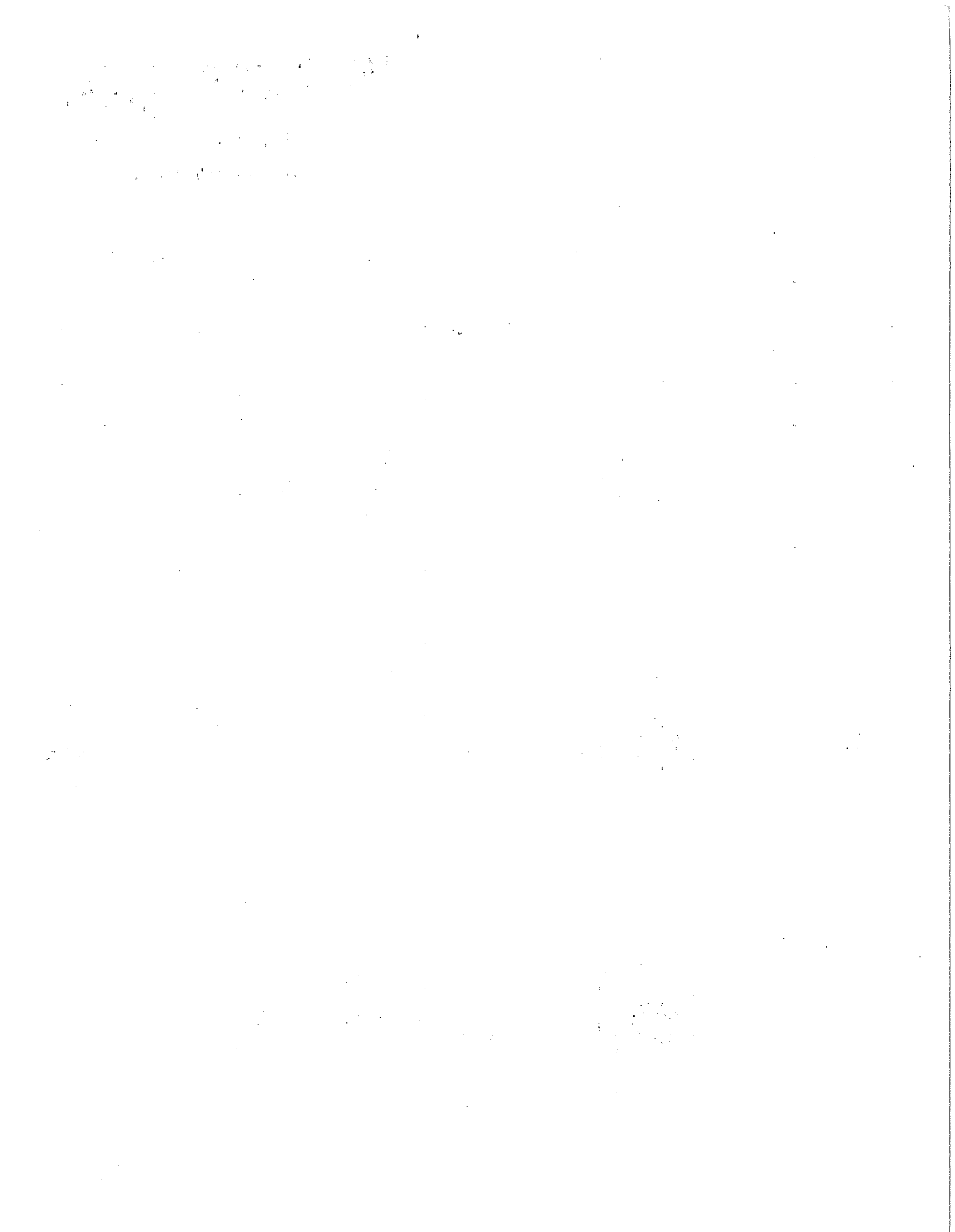
May 1993

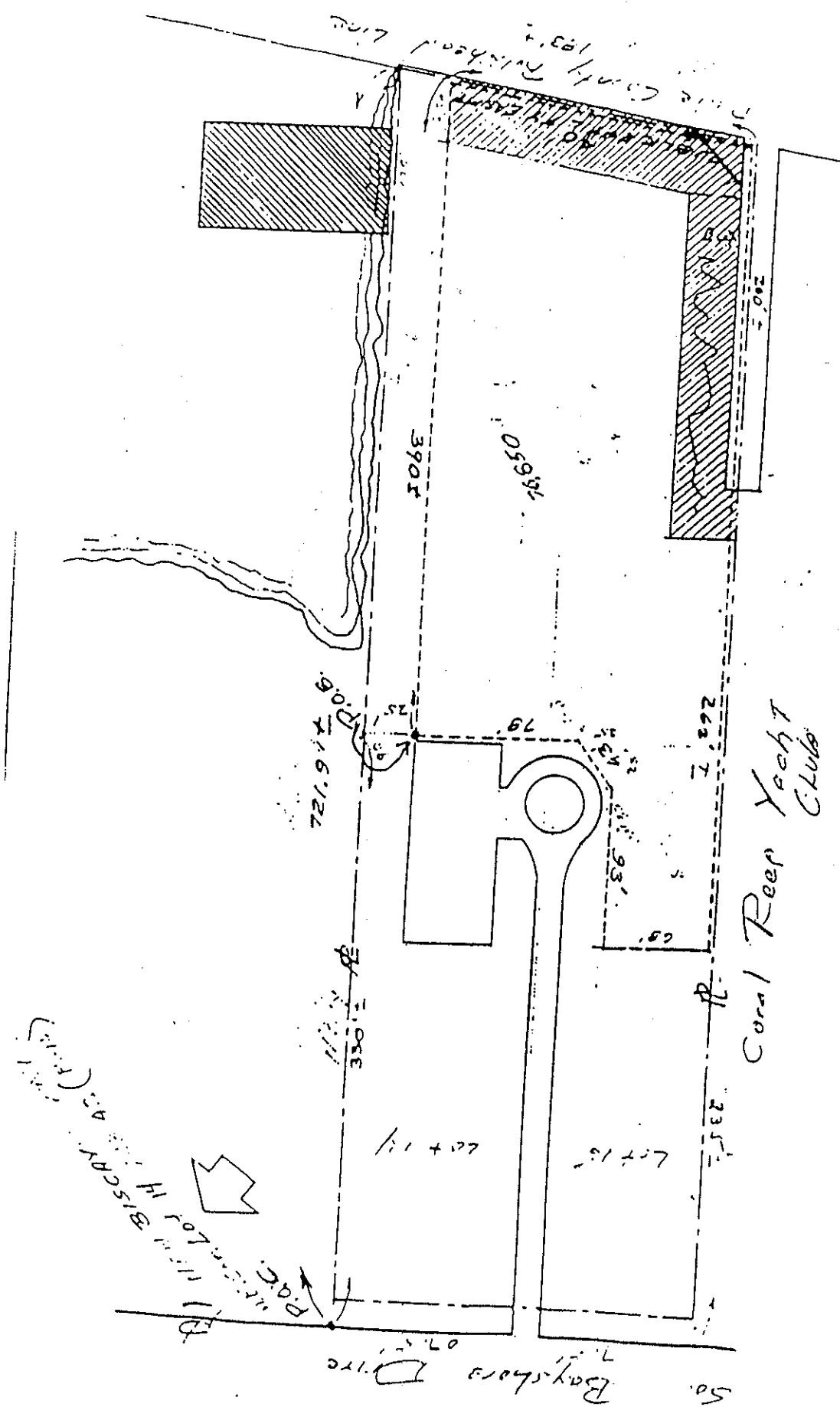
prepared by

Simpson Gumpertz & Heger Inc.
297 Broadway
Arlington, Massachusetts 02174
Tel: 617 643-2000
Fax: 617 643-2009

Comm. 93055.01

May 1993





(1/4 Sec. 15, T. 15 N., R. 15 W.)
 D.C. intersection
 Bayshore Drive

T A B L E O F C O N T E N T S

Letter of Transmittal

CONTENTS

Page

VOLUME I - Report

1.	OBJECTIVE	1
2.	SCOPE	1
3.	BACKGROUND	2
	3.1 General	2
	3.2 Hurricane Andrew	3
4.	REVIEW OF DRAWINGS	4
	4.1 Review of Drawings Representing Original Design	4
	4.2 Description of Structure	4
	4.3 Review of Drawings Representing Previously Planned Repairs	5
5.	FIELD OBSERVATIONS	7
	5.1 Hyperbolic Paraboloid Roof	7
	5.1.1 General Cracking Patterns	7
	5.1.2 Survey of Front Hypar	8
	5.1.3 Survey of Rear Hypar Cracking	9
	5.1.4 Miscellaneous Roof Structure Observations	10
	5.2 Exploratory Excavations	10
	5.3 General Condition of Stadium Structure	12
6.	LABORATORY WORK	14
	6.1 Compressive Strength Tests	14
	6.2 Chloride Content Tests	14
	6.3 Petrographic Analysis	15
7.	STRUCTURAL REVIEW	17
	7.1 Loads	17
	7.1.1 Dead Load (Self-Weight)	17
	7.1.2 Live Load	17
	7.1.3 Wind Load	18
	7.1.4 Shrinkage	19
	7.2 Finite Element Analysis	19
	7.3 Investigation of Cracking	21
	7.3.1 Cracking Strength	21
	7.3.2 Cracking in the Front Hypar	22
	7.3.2 Cracking in the Rear hypar	24
	7.4 Strength Check	25
	7.4.1 Results of Element Approach	25
	7.4.2 Results of "V" Shape Deep Beam Approach	28
	7.4.3 Diaphragm	29
	7.4.4 Buckling	29
8.	DISCUSSION	30
	8.1 General	30
	8.2 Visual Observations	30
	8.3 Laboratory Analysis	32
	8.3.1 Concrete Compressive Tests	32
	8.3.2 Chloride Content Tests	32
	8.3.3 Petrographic (Microscopic) Examination	32

8.4	Structural Review	33
	8.4.1 General	33
	8.4.2 Stress Patterns for Loads other than Wind Load	34
	8.4.3 Stress Patterns for Wind Loads	36
8.5	Strength Check	37
	8.5.1 Front Hypar Strength	37
	8.5.2 Rear hypar Strength	37
	8.5.3 Safety and Serviceability	38
8.6	Remedial Work Concepts	39

9.	CONCLUSIONS	41
----	-------------	----

VOLUME II - Illustrations and Appendices

ILLUSTRATIONS

Figures 1 to 11
 Photos 1 to 69
 Reference Drawings S-5 and S-9
 Photo Collages PS-1 to PS-6

APPENDICES

Appendix A - List of Drawings Reviewed
 Appendix B - SGH Laboratory Tests
 Appendix C - Petrographic Report
 Appendix D - Structural Review Summary Tables
 Appendix E - Cost Estimates

VOLUME III - Calculations

1. OBJECTIVE

Our objective is to determine if wind loads associated with Hurricane Andrew are the cause of cracks observed in the hyperbolic paraboloid roof, to determine whether the cracked roof structure can safely carry intended design loads, and to develop recommendations for remedial work required for the roof structure, if any.

2. SCOPE

Our conclusions are based on the following scope of work:

- 2.1 Review of structural drawings representing the original design.
- 2.2 Review of weather records for locations near the Marine Stadium during Hurricane Andrew.
- 2.3 Review of drawings for previously planned repair work.
- 2.4 Visual inspection of the structural condition of the hyperbolic paraboloid roof structure.
- 2.5 Visual inspection of the structural condition of deteriorated structural components other than the roof structure.
- 2.6 Laboratory compressive tests, chloride content tests, and petrographic analysis of concrete core samples from the roof structure.
- 2.7 Calculations to investigate the cause and significance of cracks in the roof structure and to review the adequacy of the original design.
- 2.8 Development of remedial work concepts for the roof structure.
- 2.9 Estimates of the costs of remedial work concepts.

3. BACKGROUND

3.1 General

The Miami Marine Stadium is located on Virginia Key in the City of Miami and was built in 1963. The structure is built of cast-in-place reinforced concrete, and it consists of the following four primary components: a concrete pile and grade beam system, an elevated "ground" floor, a grandstand structure, and a complex, multi-part, hyperbolic paraboloid umbrella roof (Photos 1, 2, and 3).

The grandstand is 126 ft wide by 326 ft long in plan; about 1/3 of the 126 ft width is built on piles in the water (Photo 4). The roof structure is 108 ft wide by 326 ft long in plan.

As a result of Hurricane Andrew, the City of Miami closed the Miami Marine Stadium because of concerns about the safety of the structure. The City initially claimed that the structure would require complete demolition. The claim centered on the following damage issues:

- Extensive spalling of the over-water grade beams as a result of salt-water spray from the storm (Photo 5).
- Circumferential cracks in the main roof support columns throughout their length (Photo 6, 7, and 8).
- Cracks around the heads of the main interior roof columns at the transition between the columns and the roof shell (Photo 9).
- Numerous diagonal cracks in the overhanging portion of the roof shell (Photos 10, 11, and 12).

Mr. Juan Ordonez, Structural Engineer for the City of Miami, told us that his primary concern was for the roof shell. He said that when he first inspected the structure after the storm he noticed cracking in the roof shells but was not alarmed by them. Later, facility personnel reported white staining in the cracks, and he decided to close the facility until the significance of the cracks could be evaluated.

At initial meetings between SGH and various city personnel, we reported that many of the column "cracks" were nothing more than construction joints and/or original construction patches, and that most of the other non-roof structure concerns resulted from corrosion-related deterioration, not wind effects. The City acknowledged that they received bids, just prior to the storm, for extensive repairs to concrete on pilings, grade beams, column bases, and grandstand

beams. As a result, the City reduced their claim to the roof shell only. From that time, we concentrated our investigation efforts on evaluation of the extent, cause, and age of the roof structure cracking and on evaluation of the significance of the cracking on the safety of the roof shell.

3.2 Hurricane Andrew

Hurricane Andrew struck southern Florida on 24 August 1992. By all accounts it was an intense storm, perhaps the worst to hit the United States since Camille in 1969. Dr. Peter Sparks, of Clemson University, reported in the Jan/Feb 1993 issue of Southern Building that current best estimates place the Hurricane Andrew winds, in the most severely effected areas, at 110 to 125 mph. This is lower than earlier reports of wind speeds as high as 165 mph. Spark's report of lower wind speeds is supported by a study by Reinhold, Vickery, and Powell presented at the October 1992 ACI Convention in San Juan, Puerto Rico. Virginia Key is located north of the worst wind speed area. Wind measurements made on Virginia Key, analysis of wind speed reports from other nearby areas, and testing and calibration of reporting anemometers were used by Reinhold, et al., to develop a contour plot of Hurricane Andrew maximum expected fastest mile that indicates 120 mph for the Virginia Key Area.

4. REVIEW OF DRAWINGS

4.1 Review of Drawings Representing Original Design

We reviewed drawings representing the original design of the Miami Marine Stadium prepared by Dignum Associates, Consulting Engineers, and Pancoast Ferendino, Grafton, Skeels & Burnham, Consulting Architects, both of Miami, Florida.

These drawings include Structural Drawings S-1 through S-4, S-4a, S-5, S-7, and S-9 through S-18; Drawings S-6 and S-8 are missing from the set we received. With the exception of Drawing S-4a, dated 4/30/63, all drawings are dated 4/24/63 and are stamped "AS BUILT". A list of the structural drawings we reviewed is included in Appendix A. We also received copies of Drawings C-1 and C-2, and Architectural Drawings A-1 through A-6, and A-8 through A-11. We did not make a detailed review of the Architectural Drawings.

4.2 Description of Structure

We reviewed the original structural drawings to obtain information regarding the geometry and properties of the structure including overall dimensions, member sizes, layout of reinforcing steel, and material properties of the concrete and steel.

Copies of original Drawings S-5 and S-9 are included in the illustrations section of this report. Drawing S-5 contains plan views of the roof structure. The roof consists of 8 individual concrete thin-shell structural units each comprising four hyperbolic paraboloid shells (hypar shells) joined along a centerline to form a "V"-shaped beam cross-section. Each structural unit acts as a "V"-shaped beam. Each of the eight roof units is 41 ft wide and 108 ft long. Each unit is supported by three columns, two at the back and one at the interior. The unit cantilevers 60 ft forward of the single interior column. The 8 units are tied to each other via a keyed joint filled with concrete grout which also contains steel weld tabs that restrain relative translation between adjacent units.

Drawing S-9 shows an elevation view of the stadium structure. In this report, we refer to the roof structure region between the rear columns and the interior column as the rear hypar; we refer to the overhang region as the front hypar.

On the top of the roof structure, the front hypar and the rear hypar are separated by a concrete wall, referred to as the diaphragm (Photos 13 and 14). The diaphragm is located directly above the interior column and is post-tensioned at the top.

The rear hypar is made of normal weight (145 pcf) concrete, and the front hypar is made of lightweight (115 pcf) concrete; each has a design compressive strength of 4000 psi at 28 days. The concrete is reinforced with steel reinforcing bars with a yield strength of 60,000 psi for bars greater than 5/8 inch diameter and 40,000 ksi for smaller bars.

The thickness of the shell in the rear hypar region varies from a minimum of 10 inches adjacent to the diaphragm to a maximum of 24 inches over the rear columns. There are thickened edge members containing large amounts of reinforcing steel at the ridges and valleys of the shell. The region of the rear hypar, exclusive of the edge beams, is referred to in this report as the rear hypar shell.

The thickness of the shell in the front hypar region varies from a maximum of 10 inches immediately adjacent to the diaphragm to a minimum of 3 inches over most of the area. Like the rear hypar, the front hypar includes thickened edge members containing large amounts of reinforcing steel at the ridges and valleys of the shell. The region of the front hypar, exclusive of the edge beams, is called the front hypar shell in this report.

The reinforcing steel in the front hypar shell consists of one layer of #4 bars spaced at 12 inch centers in each direction (north-south and east-west). This reinforcement is galvanized, probably because of the thinness of the concrete section, the exposure to the marine environment, and perhaps because of expectations of high permeability for the lightweight concrete.

There is currently a waterproofing coating on the roof. The coating is not indicated in the drawings. Grant Sheehan, of the City of Miami Disaster Recovery Team, told us that it was installed in 1978, and that to the best of his knowledge none existed before it.

4.3 Review of Drawings Representing Previously Planned Repairs

We reviewed a set of drawings entitled "Marine Stadium Structural Repairs, Phase II" prepared by the City of Miami, Department of Public Works and dated 25 June 1992. The drawing set contained a cover sheet and four sheets of plans, sections, elevations, details, and notes. The

purpose of our review was to understand the nature of repairs contemplated prior to Hurricane Andrew.

From our review, we identified the following as the scope of repairs represented in that package of drawings:

- Repairs to correct corrosion of reinforcing steel and associated concrete spalling at columns located at Column Coordinates E-1, C-1 and C-17.
- Repairs to correct corrosion of reinforcing steel and associated concrete spalling at pilings located at Column Coordinates J-2 and H-3.
- Repairs to correct corrosion of reinforcing steel and associated concrete spalling at foundation tie beams along Column Line E.
- Repairs to correct corrosion of reinforcing steel and associated concrete spalling at foundation tie beams along Column Lines 2, 4, 5, 6, 7, 8, 9, 10, 11, 12, 14, 15, and 16.
- Application of a surface treatment/coating to tie beams and columns along Column Lines 1 through 17, and at other areas identified by the Engineer.
- Repairs to miscellaneous concrete spalls throughout the "Grandstand Structure as directed by the Engineer."
- Repairs to slabs between Column Lines D and E where "spalls and rust stains are in existence."
- Cleaning, repair, and repainting of the corroded steel roof beams that support the suspended press box.
- Removal and replacement of handrails along the under-grandstand corridor along and between Column Lines D and E.

5. FIELD OBSERVATIONS

On 7 and 8 April 1993, Paul Kelley and Michael Brainerd, Senior Associates at Simpson Gumpertz & Heger, visited the site to inspect the condition of the roof structure, extract concrete core samples, and make exploratory concrete excavations in order to inspect the condition of the reinforcement in the front hyper shell. Kelley made additional field visits to verify information; the last visit was on 25 May 1993.

5.1 Hyperbolic Paraboloid Roof

In recording our observations, we considered north to be toward the water. The "northern portion" of the roof refers to the front hyper or overhang portion that is north of the diaphragm (Station 0' - 0"). Refer to the roof plan in Figure 1.

5.1.1 General Cracking Patterns

There is a general pattern of diagonal cracking in the overhang portion of the roof structure. From the underside, many of these cracks show signs of water leakage as evidenced by white efflorescence (Photo 15) and other staining (Photo 16). From the topside, many of the diagonal cracks in the overhang are visible in the liquid applied waterproofing (Photos 17 and 18); apparently some form of striping was applied to the cracks in the waterproofing operation. We documented the cracking patterns with several photo collages. Copies of the following photo collages are included in the illustration section of this report:

- PS-1, West Half of Roof Structure at Column Line 16
- PS-2, East Half of Roof Structure at Column Line 4
- PS-3, West Half of Roof Structure at Column Line 4
- PS-4, East Half of Roof Structure at Column Line 10

In addition to the typical diagonal cracking in the overhang portion, there is a regularly occurring crack parallel to the valleys of the rear hyper (see Photo 19). This cracking is typically on one or both sides of the valley, 2 to 4 feet above the base of the valley. Typically, there is also some minor diagonal cracking in the rear hypars adjacent to the interior column, and the rear columns (Photos 20 and 21). In general, there is no brown or gray staining on the rear hypars, but there is moderate white efflorescence in the diagonal cracks and several of the valley cracks.

5.1.2 Survey of Front Hypar

We made a subjective survey of the front hypar shells of the relative amount of underside staining, either brown, gray, or white, the extent of underside cracking, and the extent of topside cracking visible as striping in the waterproofing. Table 5.1.2 presents the results of this survey. The grading system is from 0 to 3, with 0 representing no occurrences and 3 representing the highest number of relative occurrences.

Table 5.1.2 - Visual Survey of Front Hypar Cracking

Column Line	Shell Half	Staining			Underside Diagonal Cracking	Topside Crack Striping
		Brown	Gray	White		
16	West	0	1	1-2	2	2
16	East	1	2	1-2	2	2-3
14	West	0	0-1	1-2	2	2-3
14	East	1	0	1-2	2	3
12	West	0	0	1	1-2	3
12	East	0	0	2	2-3	2
10	West	0	0	2	2	2-3
10	East	1	1	2	2	1-2
8	West	0	0	2	1-2	0
8	East	0-1	1	2	2-3	0
6	West	1	0	0-1	1	0
6	East	0	1	1-2	1-2	0
4	West	1	0	0-1	1-2	2
4	East	1	1	1	1-2	3
2	West	0	1	1	1-2	3
2	East	0	0	1	1-2	3

The staining noted in the table is primarily white efflorescence. There are isolated brown (Photo 22) and black-gray stains (Photo 23) (important because they may indicate corrosion of steel reinforcement), but these occur over less than 1% of the front hypar underside area.

We recorded the following observations from our inspection of the topsides of the front hypar:

- Crack striping is not apparent on all of the surfaces (Photo 24), but there is old appearing cracking without signs of striping. It is not clear if the crack striping was applied under the general coating or on top of it. Much of the white waterproofing on

many of the front hypar shell segments is blackened and appears to indicate that general coating erosion is exposing the striping.

- There are also severely corroded electrical conduits embedded in the concrete adjacent to the suspended press box area. The press box support beams in this area are also corroded (Photo 25).
- The diagonal cracking in the front hypar shells appears to be about every 3 ft on center. We measured 438 ft of striped crack on the west side of the front hypar Column Line 14. (Each half of the front hypar has a surface area of 1350 sq ft; 438 ft of cracking over this area corresponds to 1 ft of crack every 3.08 sq ft.)
- At several isolated locations on the overhang, there is corroded reinforcement with little or no concrete cover (Photo 26). This condition typically occurs at some of the ridge beams that run along the joints between individual roof units.
- There is a roof drain located directly over the main interior column. The drain leader is cast into the interior column. The concrete diaphragm is open over the drain to allow water from both the front and rear hypars to reach the drain (Photo 27).
- There are water overflow openings (scuppers) on each side of the front hypar shell (Photos 27 and 28). These openings are 2-1/2 inches wide by 9 inches wide. They are located 16 inches above the top of the roof structure valley, 10 ft north of the diaphragm.

5.1.3 Survey of Rear Hypar Cracking

We also made a similar survey of diagonal cracking and staining on the rear hypars. In general, diagonal cracking consists of several cracks adjacent to both the interior column and the rear columns. Staining on these cracks is moderate and always white efflorescence, and striping in the waterproofing is not as apparent as on the front hypar.

In addition, we surveyed the rear hypars for the occurrence of underside valley cracking, leakage at valley cracks, and whether reflective topside valley cracking is present on the topside. Table 5.1.3 presents the results of the valley crack survey. The table indicates that all but one unit contains valley cracking, and that on at least two units the valley cracks are striped with waterproofing on the top surface, (Photos 29 and 30).

TABLE 5.1.3 – Visual Survey of Rear Hypar Valley Cracking

Column Line	Shell Half	Underside Valley Crack	Valley Crack Staining	Topside Valley Crack
16	West	Yes	No	No
16	East	Yes	Mp	Yes
14	West	Yes	No	No

Column Line	Shell Half	Underside Valley Crack	Valley Crack Staining	Topside Valley Crack
14	East	Yes	Moderate	Yes - Striped
12	West	Yes?	No	No
12	East	Yes	No	Yes? - Striped
10	West	No	-	-
10	East	Yes	Heavy	Yes
8	West	No	-	-
8	East	No	-	-
6	West	Yes	Light	Yes - Striped
6	East	No	-	-
4	West	Yes	No	No
4	East	Yes	No	No
2	West	Yes	No	No
2	East	Yes	No	No

5.1.4 Miscellaneous Roof Structure Observations

In addition to the above, we made the following general observations of the roof structure:

- The bearing plate in the post-tensioning anchorage zone of the diaphragm end at Column Line 1 is exposed and corroded (Photo 31).
- There are cracks in the grouted joints that separate the eight individual roof structure units (Photo 32). The cracks extend from a point 3 ft from the south edge of the rear hypar to 3 ft north of the diaphragm onto the front hypar.
- There is an irregular appearing joint evident at the top of each interior column (Photos 33 and 34). It appears to be a construction joint between the top of the column and the shell.

5.2 Exploratory Excavations

We made four exploratory excavations at cracks in the front hypar shell to observe the condition of the reinforcement. The locations selected, except for Excavation E4, were at areas where waterproofing stripes were not apparent. The locations of the exploratory excavations are shown on Figure 1. We made the following observations:

Excavation E1 - Refer to Photos 35, 36, 37, and 38. There are two orthogonal layers of #4 reinforcing bars. The bar in the upper layer runs in the east-west direction and has 1 inch of clear concrete cover above it. The bar in the lower layer runs in the north-south direction. The bars are galvanized and are uncorroded. The slab thickness is 3 inches at this location. The waterproofing is cracked in the area of this excavation. We removed some of the waterproofing and measured the crack width using an optical comparator. The crack measures 0.04 inches at the concrete surface, but the crack edges are raveled so that this measurement is probably not indicative of the actual crack width below the surface.

Excavation E2 - Refer to Photos 39, 40, and 41. There are two orthogonal layers of #4 reinforcing bars. The bar in the upper layer runs in the east-west direction and has 2 inches of clear concrete cover above it. The bar in the lower layer runs in the north-south direction. The bars are galvanized and are uncorroded except for some very minor rust on the lower bar. The slab thickness is 4-5/8 inches at this location. The waterproofing is cracked in the area of this excavation. We removed some of the waterproofing and measured the crack width using an optical comparator. The crack measures 0.02 inches at the concrete surface.

Excavation E3 - Refer to Photos 42, 43, and 44. There is one #4 reinforcing bar that runs in the east-west direction and has 2-1/4 inches of clear concrete cover above it. The bar is galvanized and uncorroded. The slab thickness is 3-1/2 inches at this location. The waterproofing is cracked in the area of this excavation. We removed some of the waterproofing and measured the crack width using an optical comparator. The crack measures 0.02 inches at the concrete surface. The liquid applied waterproofing is visible in the crack below the top surface of the concrete.

Excavation E4 - Refer to Photos 45, 46, and 47. Location E4 was selected because it was adjacent to a brown stain on the underside of the roof structure. This location is also striped with waterproofing material. There are two orthogonal layers of #4 reinforcing bars. The bar in the upper layer runs in the east-west direction and has 5 inches of clear concrete cover above it. The bar in the lower layer runs in the north-south direction. The bars are galvanized and are uncorroded. The slab thickness is 7 inches at this location. The waterproofing is cracked in the area of this excavation. We removed some of the waterproofing and measured the crack width using an optical comparator. The crack measures 0.01 inches at the concrete surface.

5.3 General Condition of Stadium Structure

A comprehensive condition survey of the stadium structure below the roof was not part of the scope of our work. The observations presented below are based on a brief general examination conducted to gain a general familiarity with the condition of the entire structure.

We observed cosmetic patching at shell-beam-column joints, along the joints in the formwork, and on the top of the east-west beam at the top of the seating area. At many of the shell-beam-column joints and at many of the east-west beams, these patches are cracked and delaminated (Photo 48). At one shell-beam joint we easily removed the patch material with a hammer. The exposed substrate is covered with a blue material that probably is a bonding agent (Photo 49). These patch areas appear old, and the geometry, location, and make-up suggest they were made during the original construction period.

We observed many components with delaminated and spalled concrete over corroded reinforcement including:

- Severe and extensive corrosion of reinforcing steel and associated concrete spalling in the over-water foundation tie beams north of Column Line D (Photos 50, 51, and 52).
- Severe corrosion of reinforcing steel and associated concrete spalling in columns at Column Locations C-1 (Photos 53 and 54) and C-17 (Photo 55) and in a pier along Column Line E (Photo 56).
- Underside corrosion in the slab between Column Lines D and E (Photo 57).
- Cracking in the Grandstand slabs (Photo 58).
- Corrosion of reinforcing steel and associated delamination of concrete on the ramp slab (Photo 59).
- Corrosion of slab reinforcing steel and splitting of concrete around steel support beams in the ramp slabs (Photos 60 and 61).
- Concrete splitting and reinforcing steel corrosion in the rear, upper, east-west, grandstand beam (Photo 62). We easily removed the concrete around the splits with a mason's hammer and uncovered corroded reinforcing steel (Photo 63). We also sprayed pH indicator on the concrete and found indications of heavy carbonation.
- Corrosion of reinforcing steel and associated spalling of concrete at the top of the rear column just below where it meets the shell (Photos 64 and 65).

Many of the piles and tie beams in the over-water section of the structure have been previously repaired (Photos 66 and 67). Examination of one previous tie beam repair (Photos 68 and 69) indicates that the repair did not include the concrete around the corroding reinforcing steel.

6. LABORATORY WORK

We extracted six concrete core samples for compressive testing, chloride content testing, and petrographic analysis. Core C1 has a nominal diameter of four inches. Cores C2 through C6 have nominal diameters of two inches. The core locations are shown on Figure 1.

6.1 Compressive Strength Tests

We tested three, two-inch diameter cores for compressive strength in our laboratory. Our laboratory report is contained in Appendix B. Table 6.1 is a summary of the compressive strength test results.

Table 6.1 Results of Compressive Strength Test Results

Core	Compressive Strength (psi)
C4	4,350
C5	3,320
C6	2,810

The average compressive strength of the concrete represented by the cores is 3,500 psi. The structural drawings indicate the required compressive strength is 4000 psi.

6.2 Chloride Content Tests

We tested the remnants of the compressive test samples for chloride content. Table 6.2 is a summary of the chloride content results.

Table 6.2 Results of Chloride Content Determinations

Core	Acid-Soluble Chloride Content (Percent by Weight of Concrete)		
	1/8" from top	Middle	1/8" from bottom
C4	0.016	0.015	0.037
C5	0.022	0.010	0.052
C6	0.022	0.013	0.043

The table indicates that the chloride content in the bottom of all three core samples exceeds the generally accepted corrosion threshold of 0.03%, but that in the middle of all three samples, where the shell steel is concentrated, the chloride levels are below the corrosion threshold.

6.3 Petrographic Analysis

We engaged Steven Stokowski, Petrographer, of Stone Products Consultants, to make a petrographic analysis of the cracks in core samples we extracted during our 7 and 8 April 1993 field investigation. As noted above, we extracted three core samples through existing diagonal cracks in the front hypar shell. The cracks sampled were selected because they did not appear to have the waterproofing stripes that were observed at other cracks which certainly would have dated them as pre-hurricane. The core samples provided to Stokowski were Cores C1, C2, and C3. Core C2 was in poor condition when delivered to Stokowski because of damage to the sample that occurred while removing it from the core drill barrel.

Stokowski prepared two sets of thin section samples of the crack from each of these cores, and he examined the thin section samples in accordance with ASTM C856 - Petrographic Examination of Hardened Concrete. The purpose of his examination was to identify the characteristics of the concrete and to determine if the crack surfaces indicated the age of the cracks relative to the August 1992 occurrence of Hurricane Andrew. Stokowski also investigated the aggregate to determine if it could be the source of brown and black staining observed at some localized areas on the underside of the front hypar shell.

Stokowski's report, including detailed photographs from his microscopic examination, is included in Appendix C. A summary of Stokowski's findings is as follows:

- The general quality of the concrete is good. The binder is Portland cement; it is well hydrated, and the grain size suggests Type I cement. The bond between the cement paste and the aggregate is normal; no excessive dust was observed on the aggregate. The concrete is not air-entrained; most of the air voids are small and sub-spherical. The texture of the concrete indicates it was produced with a normal water/cement ratio, probably in the range of 0.40 to 0.44.

The coarse aggregate is a lightweight type with a nominal maximum particle size of 1/2 inch and normal aggregate grading. The lightweight aggregate is derived from a natural sandy clay, not a shale or slate; it is similar to materials processed in the Georgia coastal plain. No alkali-aggregate reactions were observed.

The fine aggregate is natural sand with quartz grains and limestone fragments, and it appears to be normally graded. No decomposed fine aggregate particles or alkali-aggregate reactions were observed. The sands were probably mined in the Miami area.

- The cracks in all three cores were initiated well before Hurricane Andrew. In two core samples, C2 and C3, the age of the crack can be dated prior to the 1978 application of the current waterproofing system since waterproofing material is found in the crack. In all three core samples, the concrete adjacent to the top of the crack is carbonated in a V-shape pattern, with the carbonation deepest at the crack. Carbonation is a reaction between carbon dioxide and cement. Carbonation is a relatively slow process that requires moisture to drive the reaction. In this instance, the extent of its occurrence in the crack is an excellent indicator that the crack is older than the August 1992 Hurricane Andrew. Similar V-shape carbonation patterns occur in the bottom of the cracks in Cores C1 and C3. There is no indication of a V-shape carbonation pattern in the bottom of Core C2, and its absence may indicate that completion of the crack extension from top to bottom in this area occurred more recently than in the other samples.
- Neither the coarse lightweight aggregate nor the fine aggregate (sand) are likely to account for the brown and black stains observed on the underside of localized areas of the hypar shell.

7. STRUCTURAL REVIEW

7.1 Loads

7.1.1 Dead Load (Self-Weight)

We used dead loads consistent with the self-weight of the roof structure in our review. The three major components of the roof structure are the front hypar, the rear hypar, and the diaphragm. The total weight of the front hypar is 155,000 pounds; the projected area of the front hypar is 2700 sf, resulting in a projected equivalent uniform load of 57 psf. The total weight of the rear hypar is 400,000 pounds; the projected area of the rear hypar is 1550 sf, resulting in a projected uniform equivalent load of 258 psf. The total weight of the diaphragm on one unit is 40,000 pounds. The self-weight load was applied in our computer model separately, not uniformly, to the slab and beam elements to more precisely define the load distribution.

7.1.2 Live Load

We reviewed the 1957 Dade County Edition of the South Florida Building Code and the 1988 Dade County Edition of the South Florida Building Code to determine the original and current prescribed live load. Both editions of the South Florida Building Code prescribe a design live load of 30 pounds per square foot (psf) for roofs. Live load reductions are not allowed for roofs.

The primary intent of the code requirement for 30 psf roof live load is to ensure that the roof has adequate strength to support ponded water in the event that the primary roof drainage system becomes clogged or if its capacity is exceeded during a heavy rain. The value of 30 psf is approximately equivalent to a 6" depth of water over the entire roof.

We determined the extent of ponded water which would occur if the primary drainage system, a 5" diameter storm leader located beneath the diaphragm at Station 0' + 0", became clogged. In such a case, water could accumulate on the roof up to an elevation of approximately 54.5', at which point it would reach the height of the storm overflows located at Station 10' on the front hypar. The maximum water depth which would occur is 1'-6" (94 psf) over the valley beam between Stations 0' and 10'. The water would result in an average live load of approximately 15 psf between these two stations. Away from these stations, the average live load would be less. Thus, the code-prescribed live load of 30 psf is very conservative for this structure.

7.1.3 Wind Load

Determination of the appropriate wind load for design of a structure like the Miami Marine Stadium is not specifically addressed by the building models in the current building codes; many times conservative estimates are used in such a design or actual scaled models are built and studied in a wind tunnel. Because this study is a limited evaluation and not a design, we opted to develop a conservative wind loading based on our review of the current codes and our interpretation of literature concerning wind loads on grandstand structures and hyperbolic paraboloid structures.

We reviewed the 1957 Dade County Edition of South Florida Building Code and of 1988 Dade County Edition of South Florida Building Code, to determine the original and current code prescribed wind load. We understand that since Hurricane Andrew, Dade County has adopted the wind load provisions of ASCE 7-88, "Minimum Design Loads for Buildings and Other Structures"; we also reviewed it.

The wind load design pressures from both editions of the South Florida Building Code are based on a basic wind speed of 120 miles per hour (mph). The wind load design pressures of ASCE 7-88 are based on a basic wind speed of 114 mph. We computed separate wind load design pressures based on the provisions of the 1957 Dade County Edition of the South Florida Building Code Edition and of the ASCE 7-88. The critical wind loadings for each code are summarized below.

1957 Dade County Edition, Southern Florida Building Code

- Upward wind load - 73 psf

ASCE 7-88

- Upward wind load - 86 psf
- "Downward" wind load - 12 psf, 17 psf, 23 psf downward on the windward side of parts with slope of up to 20 degrees, 30 degrees, and 40 degrees respectively; and 40 psf upward on the leeward side.

We also estimated the wind pressures for a 120 mph wind storm using information provided in the publications "Wind Loading in a Multiple Hyperbolic Paraboloid Shell Roof Structure" by A.J. Dutt and "Reduction of Wind Loads on a Grandstand Roof" by N.J. Cook as well as other

pertinent publications. A copy of these calculations is included in a separate volume "Condition Appraisal and Structural Review, Miami Marine Stadium Roof Structure, Miami, Florida - Volume II - Calculations." Based on a wind speed of 120 mph, the resulting wind loads, which are always upward, range from a low of 35 psf to a high of 145 psf depending on the location of the leading edge of the roof and the wind direction. These publications also indicate to us that "Downward" wind load such as that prescribed by ASCE 7-88 is not likely for a structure shape like the Miami Marine Stadium.

Based on our literature review and calculations we determined that an upward wind load of 86 psf over the entire roof as prescribed by ASCE 7-88, represents a reasonable and conservative estimate of the wind load for design and safety evaluation of the Miami Marine Stadium roof structure. Further, since this load is based on a wind speed of 120 mph, which approximates the best recent estimates of Hurricane Andrew at Virginia Key, it is also a reasonable loading to evaluate the effect of Hurricane Andrew.

7.1.4 Shrinkage

We computed the long term shrinkage of the various components of the roof structure considering the volume to surface ratio of each component and a relative humidity of 75 percent. We analyzed the roof structure for the full long-term shrinkage. To account for the beneficial effects of creep, we used a modulus of elasticity for concrete equal to 1/3 of the short term modulus.

7.2 Finite Element Analysis

We analyzed the roof structure to determine the internal stresses and forces, displacements, and external reactions resulting from dead load (self-weight), live load of 30 psf, the wind loads, and shrinkage utilizing the finite element analysis computer program NASTRAN. We modeled the reinforced concrete as a linear-elastic, homogeneous, and isotropic material. A schematic drawing of the finite element model is shown in Figure 2. The front (north) hyper, rear (south) hyper, and diaphragm are modeled with plate elements. The ridge and valley beams, front edge beam, and main column are modeled with beam elements. The back (south) corners at the shell-beam-column joint are assumed fixed against rotation and translation in all directions.

We modeled one-half of one of the eight individual shell structures. This is possible because of the symmetry of the structure. The boundary along the even-numbered column line is

modeled to reflect the continuity between the half-shell and its symmetric counterpart on the other side of the column line.

The structure was built as eight individual shell units separated by a five inch wide joint which extends from the front edge of the shell to about Station -30'; the back (southern) corners of the shells appear to be monolithic. The joint between units was left open during post-tensioning of the diaphragm beam, and was later filled with concrete. In our model, this joint is a free edge during application of post-tensioning loads.

For symmetric loads such as dead load, live load, and uniform upward pressure due to wind, the roof structure may be modeled as either free or continuous at the joint between adjacent units, with no significant difference in the results. We chose to model the joint as a free edge.

Wind loading can also cause asymmetric load cases as the result of wind blowing in the east-west direction along the length of the stadium. The wind creates upward pressure on the shell areas which slope down in the direction of the wind and downward pressure on the areas which slope up in the direction of the wind. The asymmetric wind loads which we used in our analysis represent the case where downward pressure acts on the half-hypar we modeled. When wind blows in the opposite direction, upward pressure would act on this half-hypar; however, the effect of the upward pressure on this half is not as severe as the uniform upward pressure we considered as one of our symmetric load cases. When we applied asymmetric wind loading to our model, we modelled the 5" joint between shell units as a continuous joint, with the ability to transfer axial forces, moments, and shears between units. This more accurately reflects the behavior of the structure for asymmetric loading than does the "free edge" model used for the symmetric load cases described above. As a result, the model we used to analyze downward wind pressure due to asymmetric wind does not apply to the two outermost half-hypars, where we have permanently "free" edges. However, this is acceptable because the stadium geometry is such that downward pressure could only occur on the outermost half-hypars as a result of a wind blowing from the opposite end of the stadium; shielding of the leeward shell unit by the other shell units prevents this from happening. Although not specifically addressed in the applicable South Florida Building Code, the effect of shielding in sawtooth roofs does occur and is considered in several European Building Codes.

7.3 Investigation of Cracking

Permanent stresses placed on the structure prior to Hurricane Andrew are from the effects of dead load (self-weight), post-tensioning of the diaphragm, and shrinkage. The first loads imposed on the roof structure were due to the roof structure's self-weight and the post-tensioning. As soon as the concrete was placed it began shrinking which is a normal result of the concrete curing process. Shrinkage continues for several years with virtually all of the long term shrinkage occurring within two to ten years depending primarily on relative humidity. The structural supports and differences in the rate of shrinkage between adjoining portions of the roof structure provided restraint to the shrinkage thereby causing internal forces and stresses in addition to those existing due to post-tensioning and dead load. Wind loads, including those from Hurricane Andrew caused transient stresses in the roof structure.

We determined the major principal stresses (maximum principal tensile or minimum principal compressive) and their directions for the following service load combinations:

- | | |
|--|---------|
| • Post-tensioning of diaphragm and dead load | PT+D |
| • Post-tensioning of diaphragm, dead load, and shrinkage | PT+D+Sh |
| • Post-tensioning of diaphragm, dead load, and wind | PT+D+W |

7.3.1 Cracking Strength

Concrete cracks when the tensile stress in the concrete exceeds the tensile strength of the concrete. Comparison of the major principal stresses for these three load combinations allows evaluation of the relative significance of the various loads on the tensile stresses in the roof structure.

The strength of normal weight concrete in direct tension is generally considered to range between 5 and 7-1/2 times the square root of the compressive strength. For the normal weight concrete in the rear hypar, which has a design compressive strength of 4000 psi, this equates to a tensile strength range of 315 psi to 475 psi. The direct tensile strength of lightweight concrete is approximately fifteen percent less than that of normal weight concrete. The design compressive strength of the front hypar light-weight concrete is 4000 psi, but our core tests showed an average compressive strength 3,500, with a single low of 2,810 psi. Assuming a compressive strength range of 3000 and 4000 psi, we computed the tensile strength of the front hypar concrete to range between 230 and 380 psi.

The calculations associated with our investigation of the cracking strength are included in a separate volume, "Condition Appraisal and Structural Review, Miami Marine Stadium Roof Structure, Miami, Florida, Volume III - Calculations."

7.3.2 Cracking in the Front Hypar

Figures 3 through 8 show the contour plots of the major principal stresses (maximum principal tension or minimum principal compressive) and their direction for each of the three load combinations described above. Within any element, there is a plane of action where shear stresses are zero and the axial stresses are maximum; the maximum stresses at this plane are called principal stresses. The contour plots show that the major principal stress is tension over virtually the entire front hypar shell. The magnitudes of the principal tensile stresses are significantly larger for the load combinations of PT+D and PT+D+Sh than for PT+D+W, because the upward action of the wind unloads the downward effects of self weight. The highest tensile stresses occur in the vicinity of the ridge beam under PT+D and PT+D+Sh. Table 7.3.2 shows the magnitude of the major principal stress for two longitudinal rows of elements near the ridge. The principal tensile stress near the ridge for the load combination PT+ D ranges from 39 psi to 366 psi over the length of the front hypar shell with the majority of elements showing magnitudes in the tensile strength range of 230 psi to 380 psi, which is within our estimate of cracking strength. When the effects of shrinkage are included with post-tensioning and dead load, the principal tensile stress increases to a range of 216 psi to 452 psi, which exceeds our maximum estimate of cracking strength. When the wind load is combined with post-tensioning and dead load the principal tensile stresses near the ridge reduce dramatically to a range of 4 psi to 96 psi which is well below the range of tensile strength.

Table 7.3.2 - Major Principal Stresses In Shell Near Ridge Beam Of Front Hypar

(Tensile Stress in Pounds Per Square Inch)

Element (Figure 2)	Load Combination			Element (Figure 2)	Load Combination		
	PT+D	PT+D+Sh	PT+D+W		PT+D	PT+D+Sh	PT+D+W
1133	254 +	297 +	6	1111	103	214	0
1134	272 +	275 +	12	1112	91	168	7
1135	281 +	287 +	68	1113	131	120	97
1136	301 +	324 +	40	1114	158	183	67
1137	335 +	379 +	24	1115	189	220	45
1138	366 +	452 *	11	1116	220	273 +	30
1139	334 +	418 *	6	1117	206	261 +	27
1140	311 +	397 *	4	1118	198	250 +	30
1141	294 +	381 *	6	1119	193	244 +	39
1142	279 +	367 +	12	1120	189	240 +	51
1143	267 +	355 +	19	1121	184	236 +	62
1144	257 +	345 +	28	1122	179	231 +	72
1145	248 +	336 +	38	1123	174	226	80
1146	239 +	327 +	49	1124	167	220	87
1147	234 +	320 +	63	1125	159	213	91
1148	232 +	313 +	80	1126	151	208	90
1149	228	305 +	96	1127	149	211	78
1150	202	288 +	90	1128	159	227	64
1151	177	274 +	68	1129	182	251 +	61
1152	157	254 +	55	1130	202	264 +	71
1153	111	216	43	1131	196	225	71
1154	39	266 +	35	1132	135	151	46

Note: Concrete cracking is in the range of 230 to 380 psi; values above flagged with a (+) mark exceed the lower estimate of cracking strength, and values flagged with an (*) sign exceed the upper estimate of cracking strength.

Figure 9 shows the major principal stresses, their direction, and the theoretical shape of a crack if oriented normal to the direction of the major principal stress for a transverse row of elements located approximately sixteen feet from the diaphragm for the load combination PT+D+Sh. Figure 10 shows the major principal stresses, their direction, and the theoretical shape of a crack, if oriented normal to the direction of the major principal stress for a group of elements at the front (north) corner of the front hypar for the load combination PT+D+Sh.

7.3.2 Cracking in the Rear hypar

Our field observations indicate that the rear hypar (south of the diaphragm) is largely uncracked. However, there are two types of underside cracks which appear in many of the shells: the longitudinal crack running north-south at 3 to 4 feet off of the shell centerline, and the diagonal crack at the shell-beam-column joint at the back corners.

Longitudinal (Valley) Cracks

We calculated the normal stresses in the shell, perpendicular to the longitudinal crack discussed above, for the same three service load combinations used to investigate cracking in the front hypar (see Section 7.3.2 above). Each of the load combinations causes tensile stresses at the underside of the shell along the crack; however, the magnitude of the stresses does not exceed the theoretical tensile strength of the rear hypar normal weight concrete (between 315 and 475 psi).

We also calculated the effect of a thermal gradient on the shell. A thermal gradient occurs when the sun heats up the top of an uninsulated roof slab, while the bottom of the slab remains cooler by comparison. The tensile stress at the bottom of the shell, at the location of the longitudinal crack discussed above, is approximately 570 psi from thermal gradient effects alone. This value exceeds the theoretical tensile strength of the concrete.

Diagonal Cracks

The coarse size of the element mesh used in our finite element analysis does not allow a meaningful evaluation of the behavior of the shell close to the shell-beam-column joint where diagonal cracks occur. However, these cracks are short and narrow and there is no relative vertical movement of the shell surfaces on each side of the crack. These cracks are not significant and do not warrant further study.

7.4 Strength Check

We made calculations to check the ability of the roof structure to safely carry the dead and live loads prescribed by the 1988 Dade County Edition of the South Florida Building Code and the wind loads prescribed by ASCE 7-88. We used the ultimate strength design procedures prescribed by: "Building Code Requirements for Reinforced Concrete (ACI 318-89)." The pertinent ultimate load combinations for the roof structure are:

- Post-tensioning of diaphragm plus 1.4 Dead Load plus 1.7 Live Load
- Post-tensioning of diaphragm plus 0.9 Dead Load plus 1.3 Wind Load Up
- Post-tensioning of diaphragm plus 1.05 Dead Load plus 1.275 Live Load plus 1.275 Wind Load "Down"

We used two approaches for checking the strength of the hyperbolic paraboloid roof structure. The first involved reviewing each shell and beam element for the ability to resist the internal forces determined by the finite element analysis. For this "element" approach, we evaluated the strength of the shell elements using a refined method based on the principal of minimum resistance, as advanced by A.K. Gupta in "Membrane Reinforcement in Shells," Proceedings, ASCE, V, 107, ST1, Jan. 1981. The second approach involved reviewing the hypar as a "V"-shaped deep beam, assuming that the axial force in the beams resists the full static moment and that the shell resists the full static beam shear.

Our strength check calculations are included in a separate volume, "Condition Appraisal and Structural Review, Miami Marine Stadium Roof Structure, Miami, Florida, Volume III - Calculations."

7.4.1 Results of Element Approach

Hypar Shells

Using A.K. Gupta's approach, the reinforcement is considered adequate if the following conditions are satisfied:

- $P_{nx} > F_x$
- $P_{ny} > F_y$
- $(P_{nx} - F_x)(P_{ny} - F_y) > F_{xy}^2$

where P_{nx} and P_{ny} represent the axial capacity of the reinforcement in the orthogonal directions, F_x and F_y represent the axial force in the directions of the reinforcement, and F_{xy} is the shear force. We also reviewed the effects of bending moments in the shell.

In addition to checking strength, the "element" approach provides some indication of serviceability (control of cracking) in that peak stresses at relatively small individual elements are considered. This contrasts with the "V"-shape beam approach in which the entire hypar is viewed as a unit and significant redistribution between elements is assumed. However, this "element" approach does not consider the orientation of the steel relative to the principal stress directions, nor are tensile strains in the reinforcement limited, both of which are more direct crack control methods.

Tables 7.4.1 A, B, and C, which are included in Appendix D, show the results of this review for the shell elements of the front hypar (north of Station 0') in terms of the ratios of forces obtained from the finite element analysis to resistances computed for the reinforcement. Ratios of F_x/P_{nx} , F_y/P_{ny} , M_x/M_{ax} , M_y/M_{ny} , and $(F_x)^2/(P_{nx} - F_x) (P_{ny} - F_y)$ in the 15th, 16th, 18th, 19th, and 21st columns of the tables that exceed 1.0 indicate that the reinforcement is not sufficient to meet the strength and serviceability requirements of this procedure; those values labeled "Comp" are in compression. These tables do not include perimeter elements of the shell. The perimeter shell elements overlap the edge beams, and therefore, the structural effects on these elements have been included in the review of the beams that is described below. Review of these tables shows that the load case PT+1.4D+1.7L governs. Figure 11 shows the portions of the front hypar shell where the reinforcement does not meet the strength and serviceability requirements of this procedure.

Tables 7.4.1 D, E, and F, which are included in Appendix D, show the results of this review for the rear hypar, including the perimeter elements of the shell. However, the perimeter shell elements overlap the beams at the rear hypar as they do at the front; these elements were also considered in the review of the beams. Review of these tables shows that load case PT+1.4D+1.7L governs in some areas of the rear hypar, but that load case PT+0.9D+1.3W typically governs. Ratios exceed 1.0 for many of the elements. We made additional calculations for these elements to determine whether internal forces of highly stressed elements could be redistributed to nearby, more lightly stressed, shell and/or beam elements. These calculations show that overstresses are eliminated through reasonable redistribution. These calculations are included Volume III - Calculations.

Beams

We reviewed the ability of the edge beams to resist the moments and axial loads from our finite element analysis. Tables 7.4.1 G, H, and I in Appendix C show the results for the ridge and valley beams at both the front and rear hypars.

For each beam element, the tables list both the axial force in the beam and the axial force in the shell element which overlaps the beam. If the axial forces are tensile forces, the table lists the resulting steel tensile stress in the beam based on the sum of the two axial forces. If the axial forces are compressive forces, the total force is divided by the combined concrete area of the beam and the overlapping shell element to determine the concrete compressive stress. This compressive stress value is conservative, because the effect of the reinforcing steel is neglected.

In addition to tabulating axial loads and their effects, the tables list the bending moments at each end of the beam elements. Due to the way the finite element analysis program NASTRAN works, the average of the moments at the two ends of each element is the best approximation of the actual moment in the element. The average moment for each element is also listed in the table. When the moment is listed as "N.A." or "not applicable" in the table, it is because the bending stiffness of the concrete shell is not significantly increased by the small additional beam concrete at these elements; the analysis does not assign any moment to the beam.

The "moment steel area" columns in the table list the areas of the reinforcing steel in the beams which are at the greatest distance from the neutral axis, and thus will be most effective in resisting moment. The "moment steel depth" is the depth of this "moment steel" from the compression face of the beam. These values are used to calculate the tension in the steel due to bending moment in the beams. The values are conservative for elements 3208 and 3209, which are located over the main column support at Station 0'.

Calculated moments which occur within the support area need not be considered; the maximum moment which must be considered is the moment at the face of the support.

The total tensile steel stresses, due to axial loads and bending combined, are tabulated in the last column of the table. These values are conservative for elements which are under axial compression, as the steel tension due to bending is not reduced to account for the net compression.

Tables 7.4.1 G, H, and I indicate the total steel tensile stress in the beams never exceeds 54 ksi, its ultimate capacity (including the ACI strength reduction factor). The compressive stress in the concrete due to axial loads is always less than 750 psi, a reasonable, safe ultimate limit. The compressive stress in the concrete due to bending (not tabulated) is relatively low due to the presence of compressive steel; in addition, it acts over only a small portion of the compressive concrete area.

Calculations for the beam along the front (north) edge of the shell are included in the separate volume of structural review calculations described above. The maximum total steel tensile stress is always less than its ultimate capacity of 54 ksi.

7.4.2 Results of "V" Shape Deep Beam Approach

The second approach we used to review the strength of the hypars is based on the assumption that the large axial forces resulting from the overall beam-like behavior of the roof structure are resisted by the ridge and valley beams, and that the shell resists the full static "beam" shear. We calculated the total static moment in the hypar, at various stations, due to the different factored load combinations we considered in our analysis. By dividing the total moment at a station by the depth between the ridge and valley beams at that station, we calculated the total axial force to be resisted by the beams. Our calculations indicate that the beams have sufficient capacity to resist these axial forces. The maximum tensile steel stress due to factored loads is 28.1 ksi, which occurs in the ridge beam adjacent to the diaphragm under factored dead plus live loads. This is significantly less than 54 ksi, the reduced ultimate capacity of the steel. The compressive stress in the beam concrete is always less than 1 ksi, compared with a reduced ultimate capacity of 1.9 ksi for 4 ksi concrete.

As part of this second approach, we assumed that the full static "beam" shear in the structure is resisted by the shell. We calculated the total vertical shear in the hypar, at various stations, due to the various factored load combinations we considered in our analysis. We calculated the total shear in the plane of the shell that must be resisted by the shell in order to carry this vertical shear; the total shear in the plane of the shell is greater due to the slope of the shell. We compared the shear force in the shell with its ultimate shear capacity by considering it as the web of a concrete beam, using equations provided in ACI 318. The maximum shear is always less than the shear capacity. For example, the maximum shear in the 3" thick section of the front hypar is approximately 9.6 kips per foot of shell. The capacity of this section is 10.1 kips per foot for 4 ksi concrete, and 9.7 kips per foot for 3 ksi concrete.

7.4.3 Diaphragm

We performed calculations to review the ability of the diaphragm to resist the moments, axial loads, and shears from the finite element analysis. These calculations show that the diaphragm has adequate strength. In addition, we reviewed the compressive strut at the base of the diaphragm for its ability to transfer the reaction of the main column, as determined by statics, and found it to have adequate strength.

7.4.4 Buckling

We checked the buckling resistance of the front hypar shell. We considered only the front hypar; due to its slenderness, it is much more critical than the rear hypar. We found that loads on the shell due to dead load, live load, and wind are much less than the loads required to buckle the shell, and that the normal stresses in the shell are much less than the critical buckling stress.

8. DISCUSSION

8.1 General

Our evaluation of the roof structure cracking involves visual examination to identify types and patterns of distress and cracking, laboratory analysis of samples to determine properties of the concrete, petrographic (microscopic examination) of samples to determine properties of the concrete and evidence of the age of the cracking, finite element analysis of the roof structure to determine stress patterns, calculations to evaluate the relationship of the stress patterns and our visual observations of cracking, and calculations to evaluate the safety of the structure.

8.2 Visual Observations

Our visual observations identified the occurrence of very typical crack patterns on the eight roof structure units.

All of the front hypars are experiencing widespread, closely spaced, diagonal cracking. On most of the units, these diagonal cracks contain some underside staining. The staining is predominately white efflorescence which is a salt deposit that forms when water passing through a crack picks up salts in the concrete and later evaporates from the concrete surface.

Very few of the front hypar units contain stains that would indicate corrosion of the reinforcing steel. In those units that do have such staining, it is very local, and in our physical excavations we were not able to confirm associated corrosion with adjacent reinforcing steel. The good performance of the reinforcing steel in the front hypar shells is probably due to the galvanizing on this steel.

The rear hypars contain much less cracking than the front hypars. However, there is some diagonal cracking adjacent to both the interior column and the rear columns on most units. Some of these diagonal cracks have white efflorescence on the underside, but none show any staining that would be consistent with reinforcing steel corrosion. All, but one of the rear hypars contain cracks parallel to the rear hypar valleys. In three of the eight hypars these cracks have some underside white efflorescence, but no staining that indicates reinforcing steel corrosion.

All of the hypars are coated with a white, apparently liquid applied, waterproofing coating. Our best information indicates that this coating was applied in 1978, and that prior to 1978, there

was no waterproofing on the roof structure. On six of the eight roof units, there is striping apparent in the waterproofing in a diagonal fashion, consistent with the front hypar shell diagonal cracking. On some shells this striping is distinct because of a black staining away from the stripes. Striping of this type is very common in the application of a liquid applied waterproofing as detail reinforcement to cracks, and this occurrence of striping indicates that the diagonal cracking it protects existed in 1978 and was not caused by Hurricane Andrew.

We used two of the photo collages presented in Section 5.1.1 to indicate that topside cracking evidenced by striping accounts for the majority of the cracking visible on the underside. Figure PS-5 is a markup of Figure PS-2. Cracks that can be matched together on both top and bottom surfaces are marked in red, cracks on the top without an apparent bottom mate are marked in blue, and cracks on the bottom without a top mate are marked in green. Despite the difficulty in doing the matching without a reference grid, examination of this figure clearly indicates that topside striping, which indicates a crack prior to Hurricane Andrew, accounts for the majority of the front hypar diagonal cracking visible on the bottom of the shell; only the green cracks are not explained by the topside striping evident on the photo collages. Figure PS-6, a similar markup of Figure PS-3 indicates the same.

We have not determined why striping is not visible on the front hypar region of the other two roof structure units. They also contain moderate to heavy diagonal cracking. We did examine the top surface of these apparently unstriped cracks. They do not appear recent. We extracted three core samples from cracks in apparently unstriped areas. During sampling we noted the interiors of the crack were dirty and apparently aged. In one of the core sample areas we determined with a hand lens that the waterproofing material was inside the crack, indicating that it also existed prior to the 1978 application of the waterproofing. The coating on these two units is much better in appearance, and it contains no black staining. It may be that these two "unstriped" units are striped beneath a topcoat which is just performing better than the others, or that multiple coats, and not striping were applied on these two units.

Less striping is apparent on the rear hypar regions. This is due to the less frequent occurrence of cracking. The lack of striping may also be related to the higher slopes in the rear hypars that make detail work more difficult to accomplish; the coating application on the rear is sloppy, indicating it was roughly applied. Striping was found, however, on the top surfaces of at least two of the valley cracks, clearly indicating that this type of crack existed before Hurricane Andrew.

8.3 Laboratory Analysis

8.3.1 Concrete Compressive Tests

Our tests of the compressive strength of three samples extracted from the front hypars indicates a large variation in compressive strength, from a low of 2,810 psi to a high of 4,350 psi, with an average of 3,500 psi. A sample group of three is too small to draw firm statistical conclusions, but the results indicate the concrete is inferior to the 4,000 psi strength specified on the original contract drawings. In our review, we compared stress demand to range of resistance values to account for the probable lower strength of the lightweight concrete. For purposes of studying the initiation of cracking in the concrete, a 3,000 psi concrete is only 87% as strong as a 4,000 psi concrete.

8.3.2 Chloride Content Tests

We tested the chloride content of the concrete to determine if the concrete has been contaminated by salt which can trigger corrosion of the reinforcing steel. If chloride contents are above a threshold value in the vicinity of the reinforcing steel, corrosion activity is probable in the presence of moisture and oxygen, and this information is necessary in determining possible repair procedures. A chloride content above 0.03% by weight of concrete is generally accepted as the threshold of probable corrosion. Our tests indicate that the concrete is contaminated by chloride, but the levels, adjacent to the reinforcing steel, are generally below threshold values; corrosion potential is low, and the prognosis for repairs to the concrete is good.

8.3.3 Petrographic (Microscopic) Examination

The petrographic examination of the front hypar concrete was made to determine the quality of the concrete, determine the relative age of the diagonal cracks where no waterproofing stripes were evident, and to determine if the concrete constituents are causing the local occurrences of brown and black staining.

The petrographer found the concrete to be of a generally good quality.

Examinations of the cracks in three core samples indicate that these cracks were initiated well prior to Hurricane Andrew. In two of the three samples, the petrographer reported finding waterproofing material in the top of the crack, indicating that these cracks existed prior to the

1978 application of waterproofing. This indicates that even some cracks without striping formed prior to the 1978 application of waterproofing. In all three cracks, the petrographer found evidence of a chemical reaction, carbonation, that indicates the cracks are much older than the August 1992 Hurricane Andrew. Similar carbonation was observed in the bottom of two cracks. In the remaining core, the lack of carbonation in the bottom of the crack indicates that this crack may have completed its extension from top to bottom more recently than the other two samples, and may have formed recently. This may indicate that a recent event like Hurricane Andrew could have extended some previously initiated cracks, although this is only one test and more would tests would be required to form a conclusion.

8.4 Structural Review

8.4.1 General

The Miami Marine Stadium roof is a series of eight identical concrete thin-shell structures each comprising four hyperbolic paraboloid shells (hypars) joined along a center line to form a "V"-shaped beam cross section. Each hypar carries its self-weight, live load and wind load primarily by membrane action. The overall structure acts as a "V"-shaped beam that is supported at the back corners and at the main column and extends as a cantilever beyond the main column to the front of the stadium.

Thin shells are three-dimensional structures comprising thin curved slabs, the thicknesses of which are very small compared to the overall dimensions of the structure. Because of their spatial geometry, shell structures carry loads mainly through direct compression and tension, and through in-plane shear rather than through bending and out-of-plane shear as with conventional slab and beam structures. This "membrane" behavior is similar to that of an eggshell which can resist large loads even though the shell is very thin. Typically, thin-shell structures have perimeter edge beams to carry boundary forces and transfer loads to the supports. Multiple thin shells are often joined along their boundaries at angles other than 180° to provide structural depth that will allow the overall structure to span great distances.

Hyperbolic paraboloid shells were a popular architectural and structural form in the 1950's and 60's, before sophisticated finite element analysis programs became available. Consequently, the analysis of early hypar structures was achieved by simplified manual calculations of the membrane forces in the shell and the forces in the edge members using classical membrane theory. This membrane theory approach necessarily treats the shell and edge members

separately and consequently does not properly evaluate either how the weight of the edge beam is carried or the local effects due to interaction of shell and beam immediately adjacent to the beam. The actual forces in the beams can be significantly different than those predicted by membrane theory. Bending moments in the shell were typically considered to be of secondary importance. Axial forces in the shell and edge members resulting from overall beam-like behavior were estimated based on intuitive simplifying assumptions and statics.

Current finite element analysis programs such as NASTRAN allow more realistic description and prediction of the behavior of complicated hyperbolic paraboloid structures including the effects of the spatial geometry and the inter-action of the beams and shell. Our finite element analysis of the Miami Marine Stadium roof provides accurate information regarding peak localized stresses and general stress patterns, thereby, allowing meaningful evaluation of the cracking in the roof structure.

8.4.2 Stress Patterns for Loads other than Wind Load

The first loads imposed on the roof structure included post-tensioning and the roof structure's self-weight. The effects of shrinkage were imposed on the roof structure within a few years of the completion of its construction. For the entire life of the structure, the roof has been subjected to diurnal and seasonal temperature changes.

Front Hypar Stress Patterns

Review of Figure 3 and Table 7.3.2 of major principal stress (maximum principal tension or minimum principal compression) in the front hypar shell shows that PT+D (Figure 3) causes significant tensile stress in the front hypar shell. The largest tensile stress in the front shell under PT+D is 334 psi and occurs near the ridge beam approximately 16 feet from the diaphragm. This stress is within the range of the tensile strength of the front hypar concrete, 230 to 380 psi, and indicates the possibility of cracking. The principal tensile stress decreases in the transverse direction to a minimum magnitude near the valley beam. This variation of stress is due to the overall beam-like behavior of the roof acting as a cantilever which, under dead load, results in tension in the upper portion of the structure and compression in the lower portion of the structure.

Figure 5 shows that shrinkage increases the magnitude of the principal tensile stress in both the longitudinal and transverse directions. The largest tensile stress in the front shell under

PT+D+Sh is 418 psi and occurs near the ridge beam at a distance of approximately 16 feet from the diaphragm. This stress exceeds the maximum estimated value of the tensile strength of the front hypar concrete, 380 psi.

Table 7.3.1 shows that the magnitude of the principal tensile stress at many locations in the upper portion of the hypar shell for load combinations PT+D and PT+D+Sh are in or beyond the range of the concrete tensile strength. Once the cracks form in the upper portion of the shell, stress concentrations at the crack tip exceed the tensile strength of the concrete and the crack propagates into the lower portions of the shell.

Figures 9 and 10 show the theoretical pattern of cracks drawn perpendicular to the direction of principal stress for PT+D+Sh at a location about sixteen feet from the diaphragm and at the front (north) corner of the front hypar respectively. These crack patterns closely match the typical crack patterns we observed at similar locations during our condition survey. Refer to photographic surveys PS-1 through PS-4.

Rear hypar Stress Patterns

Our calculations indicate that under the various service load combinations reviewed, the axial tension in the shell acts perpendicular to the longitudinal north-south underside crack. Under each of the service load combinations, there are significant tensile stresses at the underside of the rear hypar shell across this crack. The largest contributor to these stresses is shrinkage. However, the magnitudes of these stresses do not exceed the theoretical tensile strength of the concrete. It is possible that the crack originated at a time when the shrinkage strain had achieved the majority of its ultimate value, but before the reduction in shrinkage stresses due to creep had been fully realized.

A more plausible explanation for the longitudinal crack is restraint of thermal bowing. Thermal bowing occurs when the sun heats up the top of an uninsulated roof slab, creating a thermal gradient between the relatively warm top and cool bottom of the slab. As the top of the slab heats up, it expands, causing the slab to bow upwards. If this tendency to bow up is restrained, bending moments and associated stresses occur. When the sun creates a thermal gradient in the roof of the Marine Stadium, the tendency to bow upwards is restrained by continuity at the valley and ridge along the even-numbered column line, and to a lesser extent at the joint along the odd-numbered column line. The resulting moment leads to a tensile stress at the bottom of the slab adjacent to the ridge or valley. This stress alone exceeds the tensile

strength of the concrete at the location adjacent to the even-numbered column lines where the longitudinal cracks typically occur.

8.4.3 Stress Patterns for Wind Loads

Hurricane Andrew struck South Florida on 24 August 1992. Best estimates of the Hurricane Andrew wind speeds in the most severely effected areas are 110 to 125 miles per hour (mph). The location of the Miami Marine Stadium, Virginia Key, is north of the worst reported wind speed area. Our analysis of the effects of wind load is based on a code prescribed wind speed of 120 mph. A wind speed of 120 mph is consistent with recent studies of Hurricane Andrew fastest mile wind speeds for Virginia Key, and therefore represents a reasonable estimate of the effects of the Hurricane Andrew winds on the Miami Marine Stadium roof.

Figure 7 shows the major principal stresses in the front hypar shell due to PT+D+W. The wind load greatly reduces the principal tensile stress near the ridge beam and slightly increases the principal tensile stress near the valley beam compared to those stresses caused by post-tensioning and dead load alone. The wind load primarily counteracts the high tensile stresses caused by post-tensioning, dead load, and shrinkage. This indicates that the cracks in the front hypar are not the result of wind load during Hurricane Andrew. This is consistent with the waterproofing and carbonation observations which indicate that the overwhelming majority of the cracks predate Hurricane Andrew.

The rear hypar shell has few cracks other than the longitudinal underside cracks running north-south, and the diagonal cracks at the shell-beam-column interface at the south corner. Although a wind load such as that from Hurricane Andrew increased tensile stresses at the bottom of the slab across the longitudinal cracks, the stresses due to wind load represent only a fraction of the total stresses. The cracks are a result of the combined effects of post-tensioning, dead load, shrinkage, and thermal-induced stresses. The latter two of these are the driving forces. Although we are unable to definitely state the cause of the cracking at the shell-beam-column interface, our calculations do not support the idea of wind load being a factor. We believe that the cracking is related to shrinkage and the fixity provided by the upper grandstand beam.

8.5 Strength Check

8.5.1 Front Hypar Strength

Tables 7.4.1 A, B, and C show that the governing load case for the front hypar shell is $PT+1.4D+1.7L$. The reinforcement in the majority of the front hypar shell elements is sufficient to meet the requirements for both strength and serviceability. The axial force in the transverse direction (F_y) and the shell bending moments (M_x and M_y) are small and therefore, are of secondary importance.

The axial tension forces in the longitudinal direction (F_x) are predominant. Since the overall structure acts like a deep "V"-shaped beam, the shell participates in carrying the full static bending moment. This causes high direct tension forces in the upper portion of the shell and direct compression in the lower portion of the shell for the governing load case of $PT+1.4D+1.7L$. The reinforcement in some of the shell elements is insufficient to resist this direct tension. However, this condition is not cause for concern regarding the safety of the shell since our calculations show that the reinforcement concentrated in the beams is sufficient to resist the entire tension required to carry the full static moment and that the concrete and reinforcement in the shell are sufficient to resist the full static beam shear.

8.5.2 Rear hypar Strength

Tables 7.4.1 D, E, and F show that the critical load cases for the rear hypar shell are $PT+0.9D+1.3W$ and $PT+1.4D+1.7L$. The reinforcement in many of the shell elements is inadequate when checked using the refined method as given in the tables. However, we made additional calculations for each of the elements that appear inadequate. In these calculations, we required only that statics be satisfied, not compatibility of strain, by allowing some redistribution of the forces between the shell elements and from the shell elements to the edge beams. For example, we assumed that the entire axial tension force in the longitudinal direction for the perimeter row of elements, and sometimes the first interior row of elements, can be resisted by the reinforcement in the beams. Similarly, if a given element is overstressed in shear or in tension in the transverse direction, we assumed that some stress can be transferred to adjacent elements with excess capacity. In such a manner, we were able to find viable load paths for all of the forces from our finite element analysis. In addition, in our second review approach we found the beams adequate to resist the axial loads required to carry the full static

moment, and the shell adequate to resist the full static beam shear. Thus, we are further assured that the shell has adequate strength.

8.5.3 Safety and Serviceability

Based on the structural review, it is apparent that the original design was accomplished using analysis and design procedures that satisfied statics but not compatibility of strains. "Chapter 19 - Shells and Folded Plate Members of ACI 318" considers such an approach to be acceptable but cautions that crack control at service load levels may not be assured. In an attempt to control cracking when such an approach is used, the current edition of ACI 318 specifies that the reinforcement in the tensile zone of the shell be not less than 0.0035 times the gross area of the concrete. The reinforcement (#4@12") in the front hypar, meets this requirement where the shell thickness is less than about 4-3/4 inches. The thickness of the front hypar shell is typically less than 4-3/4 inches except for the upper portion near the juncture of the diaphragm and ridge beam. The reinforcement in the transverse (east-west) direction and some of the reinforcement in the longitudinal direction of the thicker rear hypar does not meet this crack control provision. As an additional crack control measure the current ACI 318 requires that the spacing of reinforcement not exceed three times the shell thickness in areas where the major principal stresses under factored loads exceed 3.4 times the square root of the concrete compressive strength - 215 psi assuming a compressive strength of 4000 psi. The major principal stress in the entire upper portion of the front hypar shell exceeds this limit and therefore, the spacing of the reinforcement in this area should not exceed nine inches. The size and spacing of reinforcement in the front hypar, and portions of the rear hypar, do not meet the crack control provisions of the current ACI 318. The version of ACI 318 in force at the time of the design of the Miami Marine Stadium did not contain provisions for the analysis and design of shell structures.

The analysis and design procedures used for the design of the Miami Marine Stadium achieved a safe design but one that was prone to cracking particularly at the thin lightly reinforced front hypar shell. The existing cracks in the Miami Marine Stadium roof are not cause for concern regarding the structural integrity of the roof; however, it is prudent to improve the concrete tensile strength by injecting epoxy into the cracks to better assure the continued ability of the concrete to resist shear. This will also improve the future durability of the structure by preventing direct access of the salt-laden moisture from the marine environment to the reinforcement at cracks.

8.6 Remedial Work Concepts

Our work indicates that the roof structures are safe, and that, with repairs to the cracks and the waterproofing, the roofs structures useful life can be significantly extended.

Currently the front hypar reinforcing steel is adequately resisting corrosion because it is galvanized, although the occurrence of some local brown and black staining may indicate that the effectiveness of this protection is waning. To prolong the onset of corrosion, seal the cracks, and to keep to moisture from aiding the corrosion process, replace the membrane waterproofing.

The first step in the repair process involves removing the existing waterproofing. This will be difficult because of the high slopes on the roof structure surface and because of the need to control debris near the water. Some type of human-propelled scabbler will probably prove most effective.

Once the membrane is removed, shotblast the surface to prepare for the new coating. Prior to coating, inspect the top surface for loose concrete and for cracks that require sealing.

The most effective way to seal the cracks is by epoxy injection. Since our analysis indicates the primary source of the cracking is due to a redistribution of stress from the hypar shell to hypar edge beams, the source of the cracking will not reoccur in the repair joints; therefore epoxy is a viable repair.

Epoxy injection is best done from the underside, and this will require a complex scaffolding or access system because of the geometry of the structure. With access in place, staining can also be cleaned.

The epoxy injection process requires a face seal on the bottom surface to keep the epoxy from dripping out of the crack. After injection work, the face seals must be chipped from the concrete. A new breathable coating on the underside will probably be required to disguise this work and the injected cracks, and this coating will also protect the concrete from moisture intrusion from below.

With all of the above work completed, apply a new elastomeric coating to the top surface.

We estimate that the above repairs will cost about \$1 to \$2 million. A copy of our estimate is included in Appendix E. These repairs should extend the life of the roof structure well over 10 years, except that the waterproofing may require replacement in a 5 to 10 year period.

To evaluate the cost-effectiveness of the repair solution, we made a schematic estimate of the cost to remove and replace the entire roof structure above the column tops. Because of the complexity of shoring and forming the roof structure, we retained Mr. Ted Lobus, a construction engineer with The George Hyman Co. of Baltimore, Maryland, to assist us. This estimate indicates removal and replacement to be in the range of \$4 to \$5 million. The copy of this estimate is included in Appendix E.

In addition to the above roof structure repairs which are necessary to prolong the life of the roof structure, other elements in the structure such as foundation tie beams, column bases, ramp slab supports, and grandstand beams are suffering from advanced deterioration and should be evaluated and repaired before reopening the building. A ballpark estimate of the cost of this work is \$1 million.

We have determined no direct relationship between the need for any of the above repairs and the occurrence of Hurricane Andrew.

9. CONCLUSIONS

- 9.1 The overwhelming majority of Miami Marine Stadium existed prior to 1978. We found no indications of new cracking related to Hurricane Andrew; however, we can not prove that some cracks may have been extended by the storm.
- 9.2 The diagonal cracks in the roof structure are the result of the combined effects of self-weight, post-tensioning, shrinkage, and temperature change acting on a structure that was poorly designed to control cracking.
- 9.3 The roof structure, even with the current level of cracking, is safe, but repairs to seal the cracks and restore the integrity of the waterproofing system should be made to prolong the life of the structure.
- 9.4 There are numerous instances of corrosion related deterioration on other major elements of the stadium foundation structure that are safety concerns, and these elements should be evaluated and repaired before the stadium is occupied again.

MLB1-93.ag

Comm 93055.01 – Compare Replacement To Repair

PLK – MAY REPORT

DESCRIPTION	TOTAL REPLACE COST	TOTAL REPAIR COST
DIVISION 1 – GENERAL REQUIREMENTS		
General Conditions including Mobilization	482520.00	145710.00
DIVISION 2 – SITEWORK/DEMOLITION		
Falsework, above grandstand only	1125000.00	450000.00
Controlled demolition	500000.00	-
Equipment	320000.00	20000.00
Cleanup	75000.00	12000.00
DIVISION 3 – CONCRETE		
Field built diaphragm forms	30000.00	-
Custom formwork delivered	400000.00	-
Place and strip forms	70000.00	-
Reinforcing steel, delivered	82000.00	-
Place reinforcing steel	82000.00	-
Concrete, delivered	112000.00	-
Place concrete	80000.00	-
Finish concrete	120000.00	-
Patch concrete	20000.00	17800.00
Epoxy inject cracks	-	190400.00
DIVISION 5 – METALS		
Pressbox	30000.00	-
DIVISION 7 – WATERPROOFING		
Remove existing waterproofing coating	-	71200.00
Shotblast surface to prepare for new coating	35600.00	35600.00
New elastomeric waterproofing coating	71200.00	71200.00
DIVISION 9 – FINISHES		
Powerwash underside	-	35600.00
Breathable underside coating	-	35600.00
DIVISION 16 ELECTRICAL		
New lighting	64000.00	32000.00
SUBTOTAL 02 – 16	3216800.00	971400.00
SUBTOTAL 01 – 16	3699320.00	1117110.00
20% Overhead and Profit	739864.00	223422.00
SUBTOTAL	4439184.00	1340532.00
2% Performance Bond	88783.68	26810.64
Total Construction Cost	4527967.68	1367342.64
10% Engineering Cost	452796.77	136734.26
TOTAL ESTIMATED PROJECT COST	\$4,980,764.45	\$1,504,076.90

Comm 93055.01 - Cost Estimate of Conceptual Repair Scheme

PLK - MAY REPORT

DESCRIPTION	QUANTITY	UNIT	UNIT COST	TOTAL COST	SOURCE
DIVISION 1 - GENERAL REQUIREMENTS General Conditions including Mobilization	1	Lump Sum	145710.00	145710.00	15% of DIV 01 to 16
DIVISION 2 - SITEWORK/DEMOLITION Falsework, above grandstand only	1	Lump Sum	450000.00	450000.00	40 % of Lobus Replacement
Equipment, scissorlifts	1	Lump Sum	20000.00	20000.00	PLK ESTIMATE
Cleanup	1	Lump Sum	12000.00	12000.00	PLK ESTIMATE
DIVISION 3 - CONCRETE Concrete patching, allowance	356	Sq Ft	50.00	17800.00	SGH Files
Epoxy inject cracks front hyper diagonal cracks	8000	Feet	20.00	160000.00	Jim Wilson, SPS, Boca
Epoxy inject cracks rear hyper diagonal cracks	960	Feet	20.00	19200.00	Jim Wilson, SPS, Boca
Epoxy inject rear valley cracks	560	Feet	20.00	11200.00	Jim Wilson, SPS, Boca
DIVISION 7 - WATERPROOFING Remove existing waterproofing coating	35600	Sq Ft	2.00	71200.00	Pete Emmons, SPS, Baltimore
Shotblast surface to prepare for new coating	35600	Sq Ft	1.00	35600.00	Pete Emmons, SPS, Baltimore
New elastomeric waterproofing coating	35600	Sq Ft	2.00	71200.00	Pete Emmons, SPS, Baltimore
DIVISION 9 - FINISHES Powerwash underside	35600	Sq Ft	1.00	35600.00	PLK Estimate
Breathable underside coating	35600	Sq Ft	1.00	35600.00	PLK Estimate
DIVISION 16 ELECTRICAL Floodlights	32	Each	1000.00	32000.00	Allowance
SUBTOTAL 02 - 16				971400.00	
SUBTOTAL 01 - 16				1117110.00	
20% Overhead and Profit				223422.00	
SUBTOTAL				1340532.00	
2% Performance Bond				26810.64	
Total Construction Cost				1367342.64	
10% Engineering Cost				136734.26	
TOTAL ESTIMATED PROJECT COST				\$1,504,076.90	

COMMISSION 93055.01
MARINE STADIUM SUMMARY MATERIAL QUANTITIES

QUANTITY LABEL	CONCRETE VOLUME (YDS ³)	STEEL WEIGHT (TONS)	STIRRUP(TIE) WEIGHT (TONS)
ROOF SHELL			
FRONT (LIGHT WEIGHT)	516		
FRONT SHELL BEAMS		29.6	2.4
FRONT SHELL STEEL (#4@12)		17	
DIAPHRAGM AND SPLINE BEAM		12.3	
EDGE BEAM		1.3	
BACK (NORMAL WEIGHT)	815		
BACK SHELL STEEL		44.5	
BACK SHELL BEAMS		21.2	1.6
TOTALS	1331	125.9	4
COLUMN TYPE X	131	17.5	1.6
COLUMN TYPE Y	117	10.2	1.6
OTHER COLUMNS	50.1	5	1.1
TOTAL	298.1	32.7	4.3
BEAM B20	181	5.7	0.8
BEAM XB1-XB4	163	19	2.2
UPPER GRANDSTAND GIRDER LINES 1&17	36.2	4.1	0.7
UPPER GRANDSTAND LINE 3,7,9,11,15	75.4	12	1.8
UPPER GRANDSTAND LINES 2,4,6,8,10 12,14,16	105	9.6	2.2
UPPER GRANDSTAND LINES 5&13	28.5	4.2	0.8
UPPER GRANDSTAND FRAMING	394	20.3	7.8
STEP FRAMING	18	1	
ADDITIONAL STEEL SLAB/CURB LINE D		0.9	
ADDITIONAL CONCRETE	68		
UPPER GRANDSTAND SLAB STEEL		2.7	
SHEAR CONNECTOR AT ROOF	26		3
TOTAL	1095.1	79.5	19.3
LOWER GRANDSTAND GIRDER LINE 1&17	15	0.8	0.1
LOWER GRANDSTAND GIRDERS LINES 2 THRU 16	72	6.4	0.8
SLAB ELEVATION +5	37	5.7	
LOWER GRANDSTAND FRAMING	381	18.2	8.6
ADDITIONAL CONCRETE	28		
LOWER GRANDSTAND SLAB STEEL		1.6	
CANTILEVER SLAB LINES 1&17	1.1	0.4	
BEAM B21 - CURB AROUND OPENING	9.3	0.7	
TOTAL	543.4	33.8	9.5
MEZZANINE FRAMING			
SLAB AREA BETWEEN LINES 2-4+ & 14+-16	76	6.8	
BEAM STEEL BETWEEN LINES 2-4+ & 14+-16		5	0.2
SLAB AREA BETWEEN LINES 4-6 & 12-14	62	5.5	
STEEL BEAMS 2B8&2B9		1	0.2
SLAB AREA BETWEEN LINES 6&12			
8 INCH CANTILEVER SLAB	25.8	3.4	
PAN JOIST SLAB AREA	82	4.5	
SUMMARY BEAM STEEL		3.5	0.1
STEEL 6 INCH SLAB AREA		0.2	
TOTAL	245.8	29.9	0.5

TED -

These are the material quantities for steel roof

if you have any questions don't hesitate to call.

Stan

OF MIAMI BEACH

MIAMI

MIAMI BEACH

DODGE

ISLAND

ANTARCTICA WAY

ASIA WAY

AUSTRALIA WAY

33132

LUMMUS ISLAND

MIAMI

DSR 2920
ATTACHMENT NO. 8

BISCAYNE BAY

FISHER ISLAND MIAMI DR

ISLAND MARINA

BEACH

33149

SEWAGE TREATMENT PLANT

DUCK LAKE

VIRGINIA KEY

MIAMI MARINE STADIUM



Photo 49



Photo 50



Photo 51



Photo 52



Photo 53

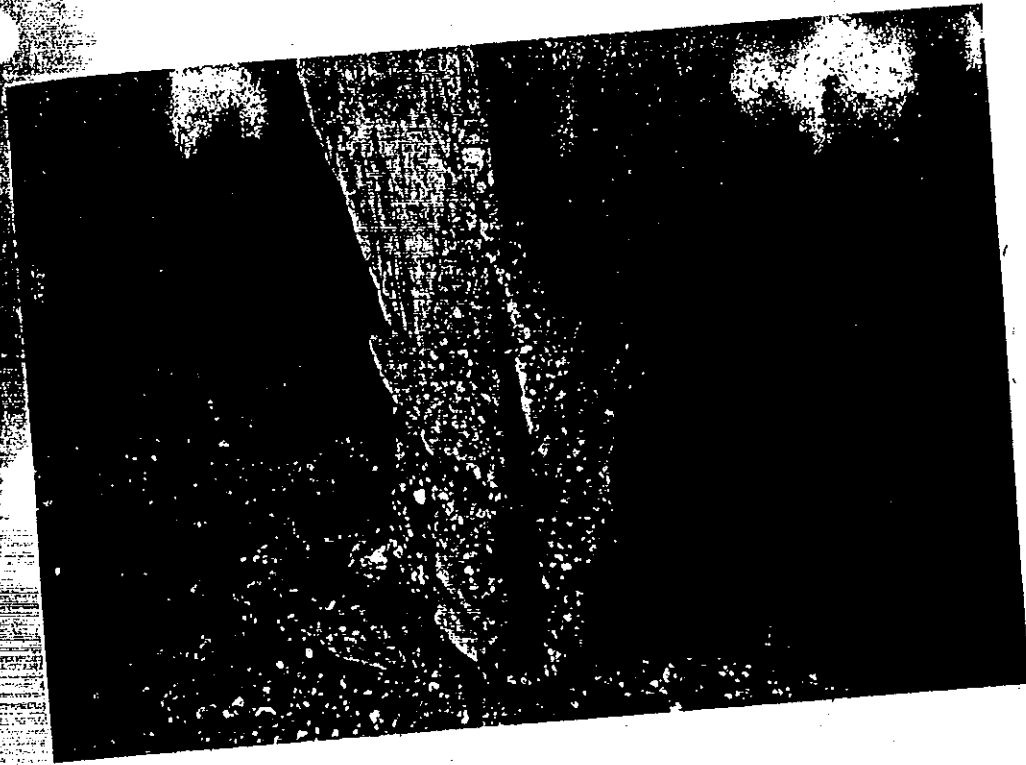


Photo 54

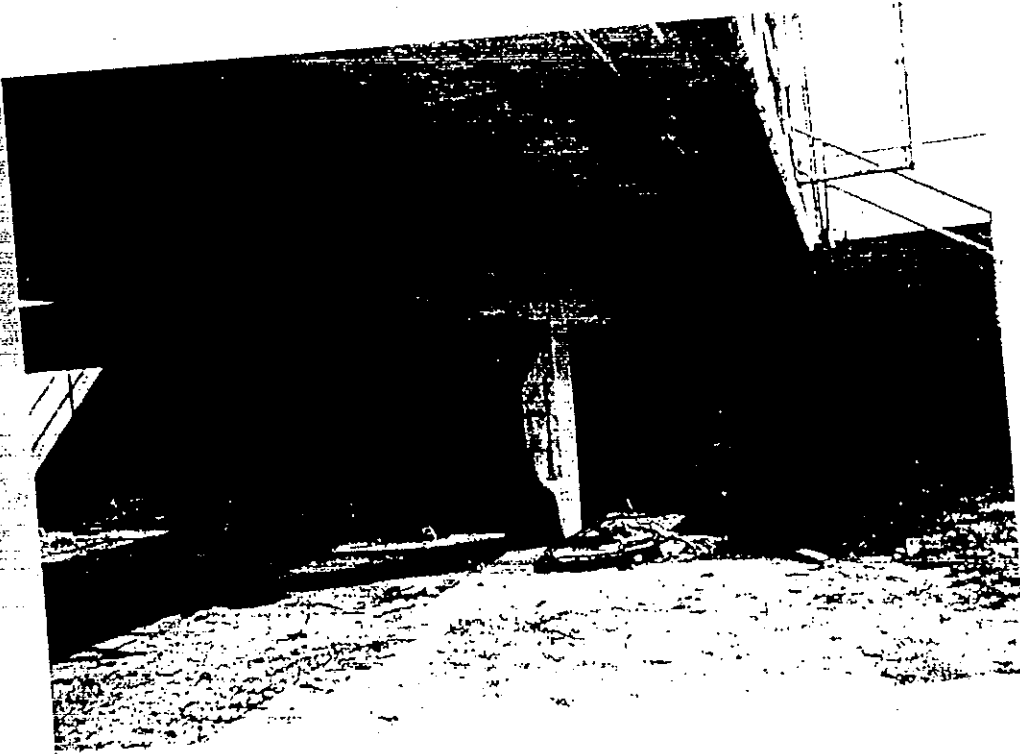


Photo 55



Photo 56

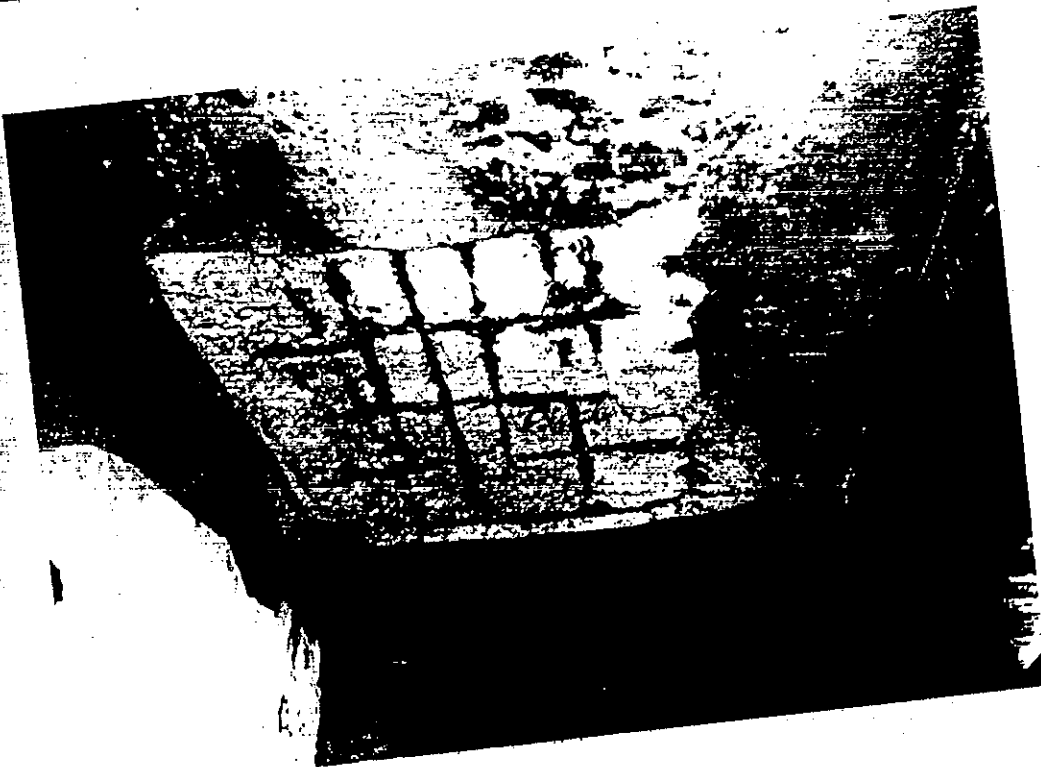


Photo 57

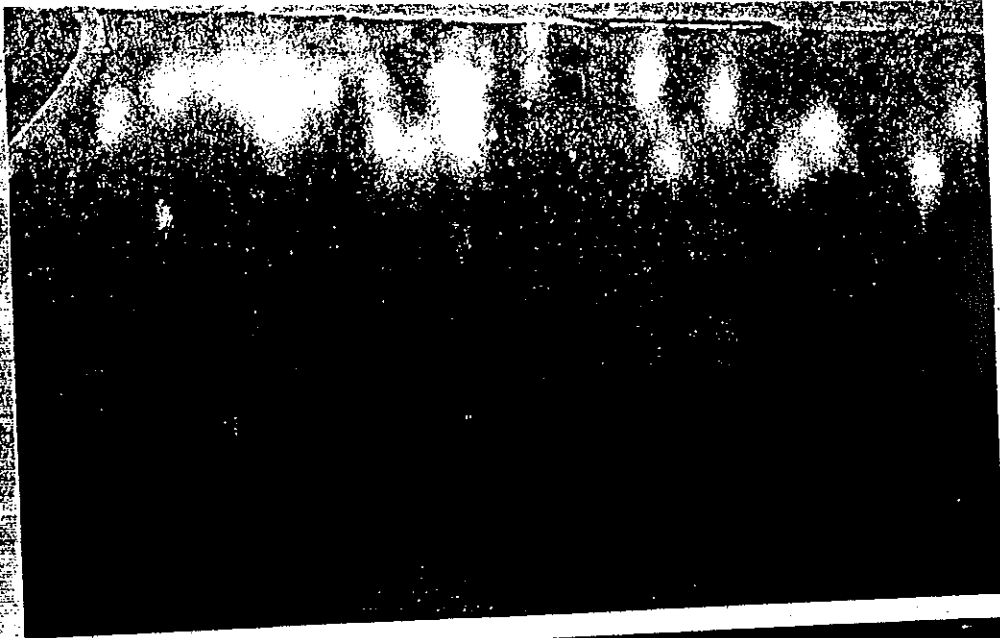


Photo 58



Photo 59



Photo 60

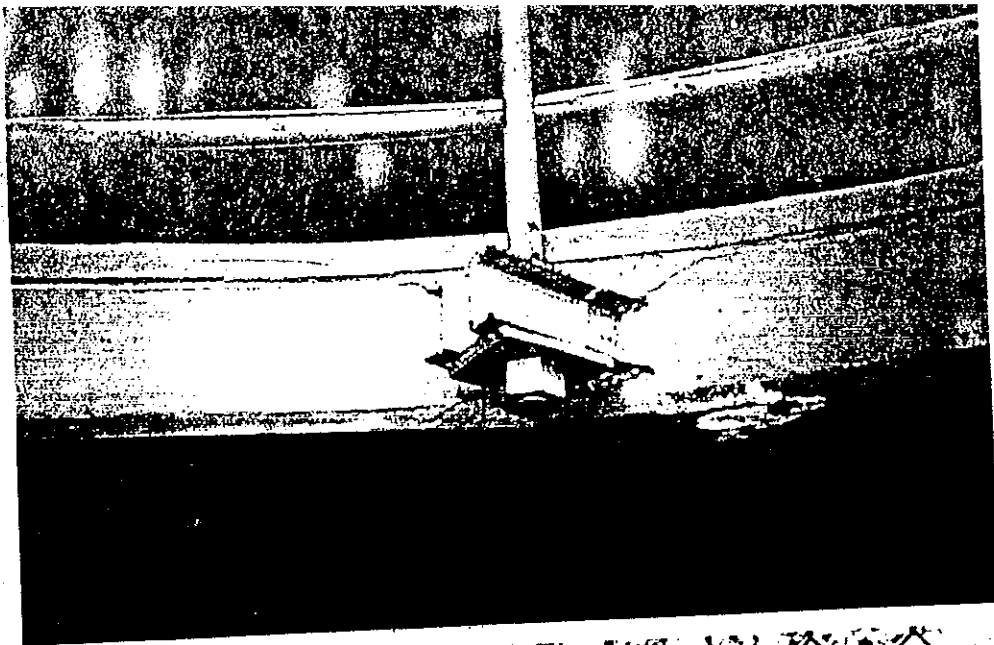


Photo 61



Photo 62



Photo 63

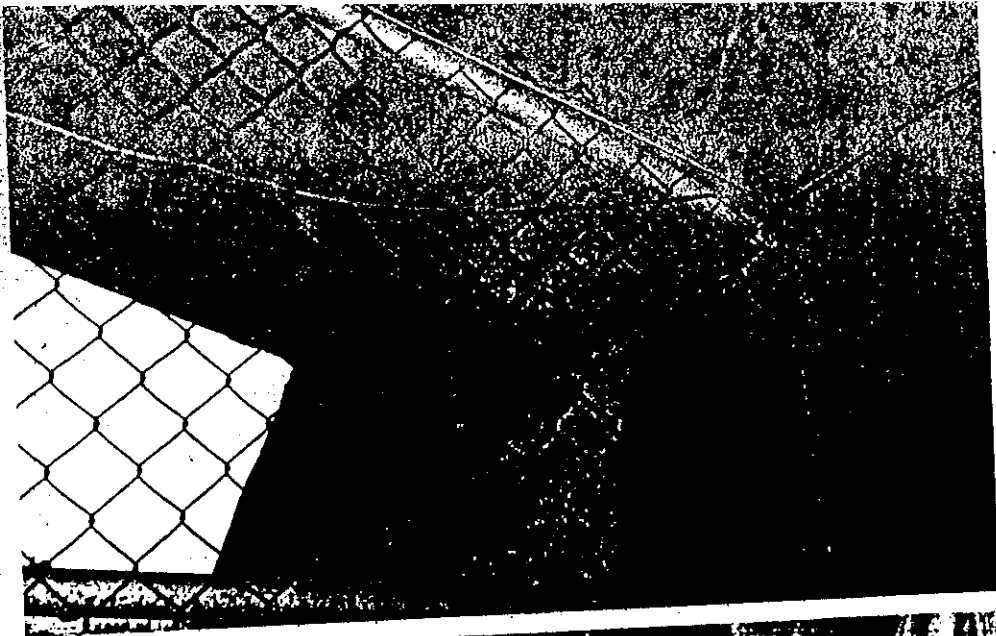


Photo 64

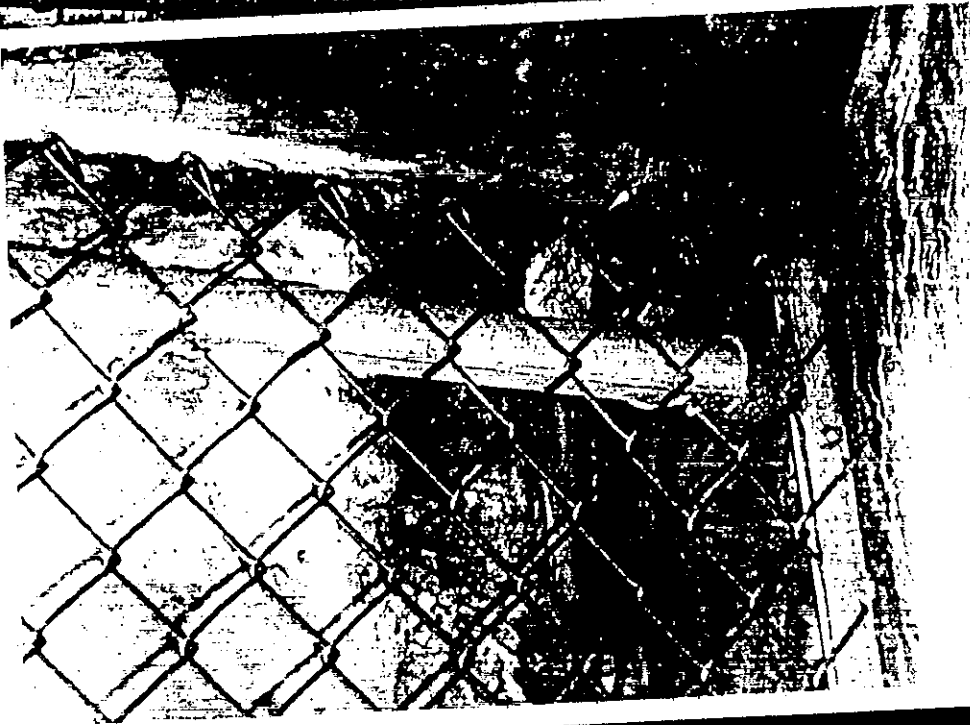


Photo 65



Photo 66

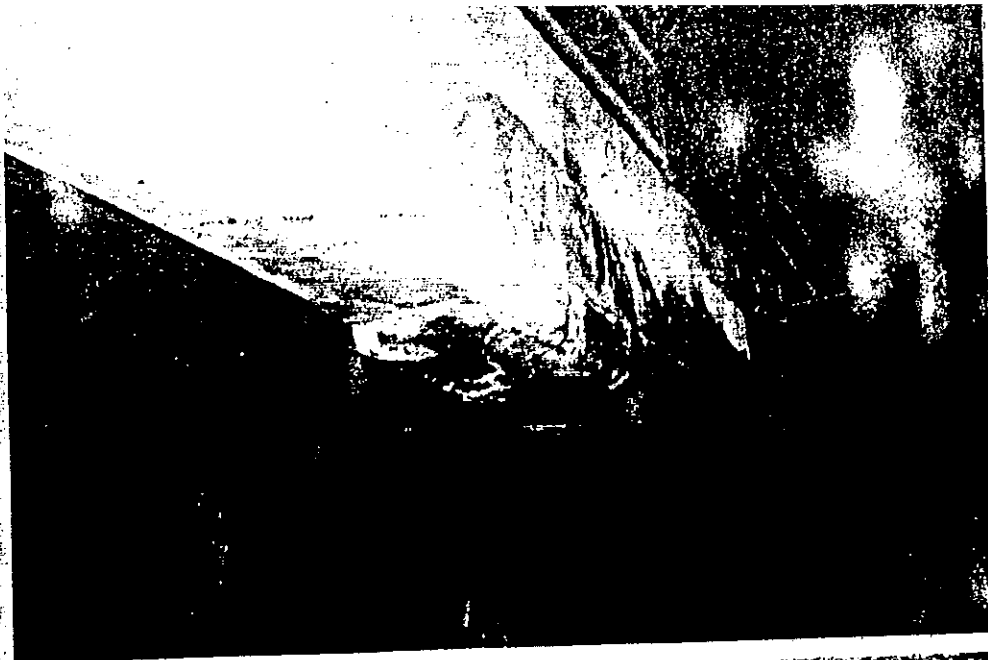


Photo 67



Photo 68

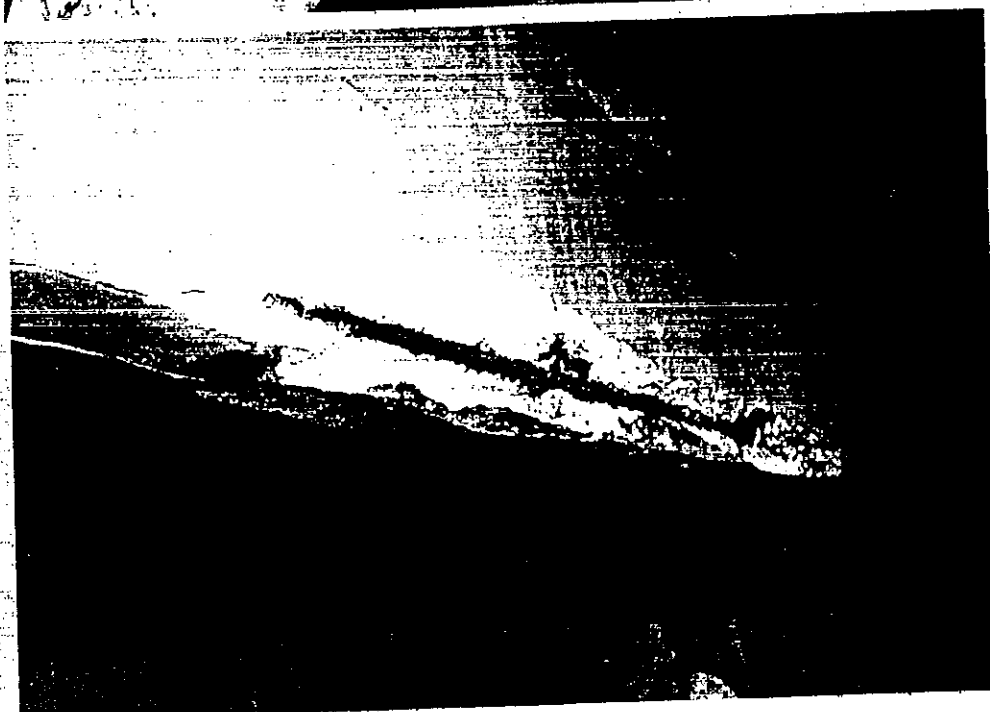


Photo 69

APPENDIX E

	A	B
1 GENERAL CONDITIONS	485,190	148,710
2 SITEWORK/DEMOLITION		
- FALSEWORK	1,125,000	435,000
- EQUIPMENT (SCISSOR LIFTS)	320,000	20,000
- DEMOLITION	500,000	-
- CLEANUP	75,000	12,000
3 CONCRETE		
- EPOXY INSTEAD CRACKS, 8000LF		200,000
- FIELDS BUILT DIAPHRAGM FORMS	30,000	-
- CUSTOM FORMWORK, DELIVERED	400,000	-
- PLACE FORMS & STRIP	70,000	-
- REINFORCING STEEL, DELIVERED	82,000	-
- PLACE REINFORCING STEEL	82,000	-
- CONCRETE, DELIVERED	112,000	3,200
- CONCRETE, PLACE/PATCH	80,000	8,000
- FINISH CONCRETE	120,000	-
- PATCH CONCRETE, SUBMITTALS	20,000	-
5 METALS		
- PRESSBOX	30,000	-
7 WATERPROOFING		
- REMOVAL EXISTING COATING	-	71,200
- PREPARE SURFACE	17,800	-
- NEW WATERPROOFING COATING	106,800	106,800
9 FINISHES		
- UNDERSLAB COATING	-	71,200
ELECTRICAL		
- SPOTLIGHTS	64,000	64,000
SUBTOTAL 02-16	3,234,600	991,400
SUBTOTAL 01-16	3,719,790	1,140,110
20% O & P	743,958	228,027
TOTAL	4,463,748	1,368,132
3% PERFORMANCE BOND	89,275	27,361
TOTAL	4,553,023	1,395,493
10% ENGINEERING & ARCH	455,302	139,551
TOTAL	5,008,325	1,535,044

City of Miami

LUIS A. PRIETO-PORTAR, PH.D., P.E.
Director



CESAR H. ODIO
City Manager


CITY OF MIAMI
MARINE STADIUM
NO. 29220

This is to clarify the City of Miami's position with reference to the DSR #29220 regarding the Marine Stadium damages caused by Hurricane Andrew on August 24, 1992.

About five years ago, the bottom portion of the lowest reinforced concrete section of the Stadium that support the first 16 rows of seats underwent major repair work. Moisture penetration through the concrete had corroded the reinforcing steel bars spalling the concrete. Following these repairs, new horizontal cracks appeared in the concrete beams not previously repaired. Also, the recently repaired beams showed new signs of deterioration.

Prior to Hurricane, Public Works was preparing to proceed with major remedial work on the lower section estimated at \$180,000. The work was not contracted when the Hurricane occurred. The storm surge from the Hurricane caused additional damage to the structure above and beyond the proposed repairs in the plans being prepared by Public Works. We have estimated that the additional damages caused by the Hurricane in the lower sections of the Stadium is approximately \$120,000 in extra work. In addition, a new cracks were detected at the top of column 2-A where the roof joins with the column. This is a complicated structural intersection.

The Marine Stadium roof structure is a unique reinforced concrete "ribbed plate" shell design supported by large sloping reinforced concrete columns. It is not possible to make a complete evaluation of the nature of this failure by visual inspection alone. It is recommended that we hire a structural consulting engineering firm to investigate the problem and make non-destructive tests. Their report should include an evaluation of the damage as well as their recommendations to correct the problems.


Economic Coord Mgr. II
Chief Engineer

MARINE STADIUM - LOCATION # 45-017

CITY OF MIAMI - MIAMI, FLORIDA
LOSS DATE - AUGUST 24, 1962

DESCRIPTION	ESTIMATE		P. O.		INVOICE		REAL & PERSONAL PROPERTY		HELD FOR DISCUSSION		TOTAL	
	AMOUNT	#	AMOUNT	#	AMOUNT	#	BLDG/CONTENTS	LEASERHOLD IMPROVE	TREES & SHRUBS REMOVAL	FLOOD	UNKNOWN	COVERED
1 FURNISH & INSTALL CHAIN FENCE			02471		\$19,973.52	6203	\$19,973.52					\$19,973.52
2 ADVERTISING EXPENSE FOR CHAIN LINK FENCING					32.50		32.50					32.50
3 WINDSTORM DAMAGE	\$500,000.00						500,000.00 (A)					500,000.00
TOTAL	\$500,000.00				\$19,973.52		\$20,006.02	\$0.00	\$0.00	\$0.00	\$0.00	\$520,006.02

NOTES: (A) HARTFORD STEAM BOILER WILL PAY UP TO \$500,000 TO REPAIR BUILDING DUE TO WINDSTORM DAMAGE - OR -
IF THE CITY OF MIAMI DECIDES TO DEMOLISH THE STRUCTURE HSB WILL PAY UP TO 5% OF DEMOLITION COSTS

DATE: 12/10/92
TIME: 07:37AM

FEDERAL EMERGENCY MANAGEMENT AGENCY
DAMAGE SURVEY REPORT
PART I - PROJECT DESCRIPTION

DSR NO: 15663
DSR:

APPLICANT NAME - MIAMI
PROJECT TITLE - ELECTRICAL DAMAGE
DAMAGED FACILITY - MARINE STADIUM
LOCATION - 3601 RICKENBACKER CAUSWAY

COUNTY - DADE
INSPECTION DATE: 10/29/92
DISASTER NO: 0955
P.A. ID 025-45000
CATEGORY F
PROJECT NO: 699
% COMPLETE 1
WORK ACCOM BY: FORCE ACCT CONT

DAMAGE DESCRIPTION AND SCOPE OF ELIGIBLE WORK:

RE-AIM EXSISTING LIGHT FIXTURES. REPLACE BROKEN AND/OR MISSING FIXTURES. REPLACE MISSING O.N. CONDUCTORS ON PARKING LOT.
REPLACE/REPAIR ENTRANCE SIGN. LOSS DUE TO HIGH WINDS & WATER DAMAGE.

RECOMMENDATION BY INSPECTOR	INSP NO.	AGENCY	ELIGIBLE	F.O
FEDERAL - GEORGE G. REAGAN	4442	TAC	Y	
STATE -				
LOCAL - FRANK K. ROLLASON				

PART II - ESTIMATED COST OF PROPOSED WORK

ITEM	CODE	MATERIAL AND/OR DESCRIPTION	UNIT	QTY	UNIT PRICE	COST
1	7531	LIGHTING, RE-AIM 1-4 LIGHTS/POLE	EA	21.00	\$40.00	\$840.00
2	7538	LIGHT, METAL HALIDE FLOOD, 1500	EA	5.00	\$311.00	\$1,555.00
3	9999	WIRE & FIXTURES	LS	1.00	\$17,212.00	\$17,212.00
4	9999	FRONT ENTRANCE SIGN	EA	1.00	\$7,000.00	\$7,000.00
5	9999	BROKEN CONDUIT CONN.	EA	4.00	\$26.25	\$105.00
6	7539	LIGHTING, LENS COVER	EA	4.00	\$35.00	\$140.00

EXISTING INSURANCE TOTAL: \$26,852.00
TYPE G AMOUNT: DEDUCT:

PART III - FLOOD PLAIN MANAGEMENT/HAZARD MITIGATION REVIEW

DOES OR AFFECTS FLOOD- FLOODPLAIN % DAMAGE DISASTER LAND USE FPM RECOMMEN-
PLAIN OR WETLAND: F LOCATION: 1 1 HISTORY: Y U3 - D3 DATION: 5

PART IV - FOR FEMA USE ONLY

AMOUNT ELIGIBLE SPECIAL CONSIDERATIONS FLOODPLAIN REV. NO. WORKSITE
.00 S
INSURANCE COMMITMENT REQUIRED SUPP# DATE PAPPED
TYPE AMOUNT YEARS

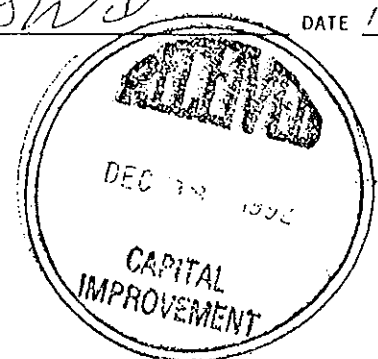
COMMENTS/CHANGES

SUSPEND PENDING SETTLEMENT OF INSURANCE. SEPERATE ITEMS 1 AND 2 TO FEMA CODE. ITEM 3 HAS BEEN CORRECTED TO CORRECT UNIT PRICES.

FEMA REVIEWER [Signature] DATE 12/11/92

DSR NO: 15663

COPIED
SUSPENDED



DAMAGE SURVEY REPORT
PART I - PROJECT DESCRIPTION

APPLICANT NAME - MIAMI
PROJECT TITLE - RECREATIONAL FACILITY
DAMAGED FACILITY - MARINE STADIUM
LOCATION - RICKENBACKER CAUSEWAY MIAMI, FLORIDA

COUNTY - DADE
INSPECTION DATE: 10/14/92
DISASTER NO: 0955
P.A.ID 025-45000
CATEGORY G
PROJECT NO: 704
% COMPLETE 10
WORK ACCOM BY: FORCE ACCT CONT

DAMAGE DESCRIPTION AND SCOPE OF ELIGIBLE WORK:

RECREATIONAL FACILITIES DAMAGED BY STORM INCIDENT. RESTORE FACILITY BY REPAIR OR REPLACEMENT AS LISTED BELOW. NUMEROUS TREES BLOWN OVER AND DAMAGED AND DOCK DAMAGED BY STORM. REPLACE OR RESTAND TREES AND REBUILD DOCK TO PRE-DISASTER CONDITION

RECOMMENDATION BY INSPECTOR	INSP NO.	AGENCY	ELIGIBLE	F.O
FEDERAL - THOMAS PORTER	4179	FEMA	Y	
STATE - RICHARD S WILLIAMS	4727	FLDER		
LOCAL - FRANK ROLLASON				

PART II - ESTIMATED COST OF PROPOSED WORK

ITEM	CODE	MATERIAL AND/OR DESCRIPTION	UNIT	QTY	UNIT PRICE	COST
1	1033	DEBRIS (HAZARD TREE LIMBS/PER TREE)	EA	10.00	\$20.00	\$200.
2	1030	DEBRIS (TREES 8-18")	EA	13.00	\$50.00	\$650.
3	9999	RESTAND 8-18" TREE	EA	8.00	\$526.00	\$4,208.
4	1014	DEBRIS (TREES & LIMBS, CONCENTRATED)	CY	20.00	\$6.00	\$120.
5	9999	REPLACEMENT 15' TREES	EA	13.00	\$225.00	\$2,925.
6	7162	PIERS, DECKING 2"X8"	MBF	.16	\$1,000.00	\$160
7	7161	PIERS, STRINGER 2"X12"	MBF	.72	\$1,000.00	\$720
TOTAL:						\$8,983

PART III - FLOOD PLAIN MANAGEMENT/HAZARD MITIGATION REVIEW

IN OR AFFECTS FLOOD- PLAIN OR WETLAND: F	FLOODPLAIN LOCATION: 1	% DAMAGE 1	DISASTER HISTORY: U	LAND USE U3 - D3	FPM RECOMMEN- DATION: 5
---	---------------------------	---------------	------------------------	---------------------	----------------------------

PART IV - FOR FEMA USE ONLY

AMOUNT \$8,983.00	ELIGIBLE Y	SPECIAL CONSIDERATIONS M1S1F1	FLOODPLAIN REV. NO.	WORKSITE
----------------------	---------------	----------------------------------	---------------------	----------

INSURANCE COMMITMENT REQUIRED

TYPE	AMOUNT	YEARS
------	--------	-------

SUPP# DATE PAPPED



FEMA REVIEWER E. Mann DATE 11/6/92

DATE: 11/05/92
TIME: 05:02PM

FEDERAL EMERGENCY MANAGEMENT AGENCY
DAMAGE SURVEY REPORT
PART I - PROJECT DESCRIPTION

NO: 29220
SUPP TO DSR:

APPLICANT NAME - MIAMI

COUNTY - DADE

PROJECT TITLE - REPAIR OF CONCRETE SUBSTRUCTURE ELEMENTS
DAMAGED FACILITY - MARINE STADIUM (DSR / 3 OF 3)

INSPECTION DATE: 09/05/92

DISASTER NO: 0955
P.A. ID 025-45000

LOCATION - 3601 RICKENBACKER CAUSEWAY, MIAMI

CATEGORY E
PROJECT NO: 599
% COMPLETE 1
WORK ACCOM BY: CONTRACT

DAMAGE DESCRIPTION AND SCOPE OF ELIGIBLE WORK:

HIGH WAVES CAUSED CONCRETE SPALLING OF SUBSTRUCTURE MEMBERS. REPAIR GRADE BEAMS BY REMOVING DETERIORATED CONCRETE, SANDBLASTING, OF CONCRETE AND REINFORCEMENT, REPAIRING DAMAGED REINFORCEMENT, APPLING OF BONDING AGENT, AND SURFACE SEALER. REPAIR PILES BY PROVIDING PILE JACKETS TO BE FILLED WITH EPOXY GROUT MORTAR.

RECOMMENDATION BY INSPECTOR	INSP NO.	AGENCY	ELIGIBLE	P.O
FEDERAL - YOSRY NASR	4414	TAC	Y	
STATE -				
LOCAL - FRANK K. ROLLASON				

PART II - ESTIMATED COST OF PROPOSED WORK

ITEM	CODE	MATERIAL AND/OR DESCRIPTION	UNIT	QTY	UNIT PRICE	COST
1	9999	CONCRETE, REMOVAL	CP	110.00	\$45.00	\$4,950.00
2	9999	REINFORCEMENT REHABILITATION	LF	180.00	\$12.00	\$2,160.00
3	9999	CONCRETE, REPLACEMENT	CP	110.00	\$125.00	\$13,750.00
4	9999	SURFACE SEALER, REPLACEMENT	SP	400.00	\$1.75	\$700.00
5	9999	PILE REPAIR	EA	6.00	\$1,200.00	\$7,200.00
					TOTAL:	\$28,760.00

EXISTING INSURANCE

TYPE G AMOUNT: DEDUCT: TOTAL: \$28,760.00

PART III - FLOOD PLAIN MANAGEMENT/HAZARD MITIGATION REVIEW

IF OR AFFECTS FLOOD- FLOODPLAIN & DAMAGE DISASTER LAND USE FPM RECOMMEN-
PLAIN OR WETLAND: W LOCATION: 1 HISTORY: U U3 - D3 DATION: 5

PART IV - FOR FEMA USE ONLY

ELIGIBLE SPECIAL CONSIDERATIONS FLOODPLAIN REV. NO. WORKSITE
S

INSURANCE COMMITMENT REQUIRED

TYPE AMOUNT YEARS SUPP/ DATE PAPPED

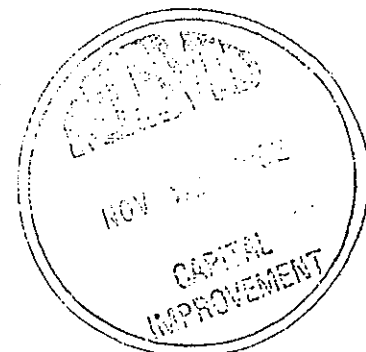
REMARKS/CHANGES

EXPEND PENDING SETTLEMENT OF INSURANCE.

FEMA REVIEWER B. Mann DATE 11/16/92

DSR NO: 29220

**COPIED
SUSPENDED**



DATE: 05/11/93
 TIME: 11:39AM

FEDERAL EMERGENCY MANAGEMENT AGENCY
 DAMAGE SURVEY REPORT
 PART I - PROJECT DESCRIPTION

DSR NO: 29220
 SUPP TO OSR:

APPLICANT NAME - MIAMI
 PROJECT TITLE - REPAIR OF CONCRETE SUBSTRUCTURE ELEMENTS
 DAMAGED FACILITY - MARINE STADIUM (OSR # 3 OF 3)
 LOCATION - 3601 RICKENBACKER CAUSEWAY, MIAMI

COUNTY - DADE
 INSPECTION DATE: 09/05/92
 DISASTER NO: 0955
 P.A.ID 025-45000
 CATEGORY E
 PROJECT NO: 599
 % COMPLETE 1
 WORK ACCOM BY: CONTRACT

DAMAGE DESCRIPTION AND SCOPE OF ELIGIBLE WORK:

HIGH WAVES CAUSED CONCRETE SPALLING OF SUBSTRUCTURE MEMBERS. REPAIR GRADE BEAMS BY REMOVING DETERIORATED CONCRETE, SANDBLASTING, OF CONCRETE AND REINFORCEMENT, REPAIRING DAMAGED REINFORCEMENT, APPLYING OF BONDING AGENT, AND SURFACE SEALER. REPAIR PILES BY PROVIDING PILE JACKETS TO BE FILLED WITH EPOXY GROUT MORTAR.

RECOMMENDATION BY INSPECTOR	INSP NO.	AGENCY	ELIGIBLE	F.O
FEDERAL - YOSRY NASR	4414	TAC	Y	
STATE -				
LOCAL - FRANK K. ROLLASON				

PART II - ESTIMATED COST OF PROPOSED WORK

ITEM	CODE	MATERIAL AND/OR DESCRIPTION	UNIT	QTY	UNIT PRICE	COST
1	9999	CONCRETE, REMOVAL	CF	110.00	\$45.00	\$4,950.00
2	9999	REINFORCEMENT REHABILITATION	LF	180.00	\$12.00	\$2,160.00
3	9999	CONCRETE, REPLACEMENT	CF	110.00	\$125.00	\$13,750.00
4	9999	SURFACE SEALER, REPLACEMENT	SF	400.00	\$1.75	\$700.00
5	9999	PILE REPAIR	EA	6.00	\$1,200.00	\$7,200.00
6	5901	ESTIMATED INSURANCE PROCEEDS, DEDUCT.	LS	1.00	\$-28,760.00	\$-28,760.00
TOTAL:						\$.00

EXISTING INSURANCE
 TYPE G AMOUNT: DEDUCT:

PART III - FLOOD PLAIN MANAGEMENT/HAZARD MITIGATION REVIEW

IN OR AFFECTS FLOOD- FLOODPLAIN % DAMAGE DISASTER LAND USE FPM RECOMMEN-
 PLAIN OR WETLAND: W LOCATION: 1 HISTORY: U U3 - D3 DATION: 5

PART IV - FOR FEMA USE ONLY

AMOUNT ELIGIBLE SPECIAL CONSIDERATIONS FLOODPLAIN REV. NO. WORKSITE
 \$.00 N MIS1F102

INSURANCE COMMITMENT REQUIRED SUPP# DATE PAPPED
 TYPE AMOUNT YEARS

DATE: 11/05/92
TIME: 10:36AM

FEDERAL EMERGENCY MANAGEMENT AGENCY
DAMAGE SURVEY REPORT
PART I - PROJECT DESCRIPTION

DSR NO: 11189
SUPP TO DSR:

APPLICANT NAME - MIAMI
PROJECT TITLE - REPLACEMENT OF CHAIN LINK FENCE
DAMAGED FACILITY - MARINE STADIUM (DSR 1 OF 3)
LOCATION - 3601 RICKENBACKER CAUSEWAY, MIAMI

COUNTY - DADE
INSPECTION DATE: 09/04/92
DISASTER NO: 0955
P.A.ID 025-45000
CATEGORY E
PROJECT NO: 599
% COMPLETE 1
WORK ACCOM BY: CONTRACT

DAMAGE DESCRIPTION AND SCOPE OF ELIGIBLE WORK:

REPLACE 1100 LF OF CHAIN LINK FENCE OUTSIDE THE STADIUM DAMAGED BY HIGH WINDS.

RECOMMENDATION BY INSPECTOR	INSP NO.	AGENCY	ELIGIBLE	F.O
FEDERAL - YOSRY NASR STATE - LOCAL - EDWARD PIDERMAN	4414	TAC	Y	

PART II - ESTIMATED COST OF PROPOSED WORK

ITEM	CODE	MATERIAL AND/OR DESCRIPTION	UNIT	QTY	UNIT PRICE	COST
1	7081	FENCE, 6' CHAINLINK, REPLACE	LF	1100.00	\$6.00	\$6,600.00
TOTAL:						\$6,600.00

PART III - FLOOD PLAIN MANAGEMENT/HAZARD MITIGATION REVIEW

IN OR AFFECTS FLOOD- PLAIN OR WETLAND: W	FLOODPLAIN LOCATION: 4	% DAMAGE 1	DISASTER HISTORY: U	LAND USE U3 - D3	FPM RECOMMEN- DATION: 5
---	---------------------------	---------------	------------------------	---------------------	----------------------------

PART IV - FOR FEMA USE ONLY
SPECIAL CONSIDERATIONS

AMOUNT	ELIGIBLE	FLOODPLAIN REV. NO.	WORKSITE
\$6,600.00	Y		

INSURANCE COMMITMENT REQUIRED
TYPE AMOUNT YEARS

SUPP# DATE PAPPED



FEMA REVIEWER

E. Mann

DATE

11/6/92

DSR NO: 11189

PART I - PROJECT DESCRIPTION

APPLICANT NAME/COUNTY: CITY OF MIAMI
 3. PA IDENTIFICATION NO.: 025-45000
 10. PROJECT TITLE: REPAIR OF CONCRETE SUBSTRUCTURE ELEMENTS
 4. INSPECTION DATE: 9/5/92
 5. PROJECT NO.: 599
 11. DAMAGED FACILITY: MARINE STADIUM (DSR # 3 OF 3)
 6. % COMPLETE: 1
 7. WORK ACCOM BY: F (C) FC
 12. FACILITY LOCATION: 3601 RICKENBACKER CAUSEWAY, MIAMI
 8. FINAL DSR: YES
 9. CATEGORY: E
 13. DAMAGE DIMENSIONS/DESCRIPTION/SCOPE OF ELIGIBLE WORK:
 DIMENSIONS: HIGH WAVES CAUSED CONCRETE SPALLING OF SUBSTRUCTURE MEMBER.
 DESC/SCOPE: REPAIR GRADE BEAMS BY REMOVING DETERIORATED CONCRETE, SANDBLAST OF CONCRETE AND REINFORCEMENT; REPAIR DAMAGED REINFORCEMENT APPLYING OF BONDING AGENT, AND SURFACE SEALER. REPAIR PILE BY PROVIDING PILE JACKETS TO BE FILLED WITH EPOXY GROUT MORTAR.

14. INSP NO.: 4414
 15. NAME OF FEDERAL INSPECTOR (Print): YOSBY NASR
 16. AGENCY CODE: []
 RECOMMENDATION: Y (N)
 ATTACHMENTS: 8
 18. INSP NO.: []
 NAME OF STATE INSPECTOR (Print): NONE
 AGENCY CODE: []
 RECOMMENDATION: Y (N)
 ATTACHMENTS: []
 19. NAME OF LOCAL REPRESENTATIVE (Print): FRANK KOUASSO [Signature]
 CONCUR: Y (N)
 ATTACHMENTS: 1

PART II - ESTIMATED COST OF PROPOSED WORK

ITEM	CODE	MATERIAL AND/OR DESCRIPTION (a)	UNIT OF MEAS (b)	QUANTITY (c)	UNIT PRICE (d)	COST (e)
1	9999	CONCRETE, REMOVAL	CF	110	45	4,950.0
2	9999	REINFORCEMENT REHABILITATION	LF	180	12	2,160.0
3	9999	CONCRETE, REPLACEMENT	CF	110	125	13,750.0
4	9999	SURFACE SEALER, REPLACEMENT	SF	400	1.75	700.0
5	9999	PILE REPAIR	EA	6	1,200	7,200.0
6						
7						
8						

20. EXISTING INSURANCE TYPE - F: \$ NONE (G) = NOT SETTLED
 21. TOTAL \$

PART III - FLOODPLAIN MANAGEMENT/HAZARD MITIGATION REVIEW

22. IN OR AFFECTS FLOODPLAIN OR WETLAND: F (W) N
 23. FLOODPLAIN LOC: 1 2 3 4 5
 24. % DAMAGE: (1) 2 3 4
 25. DISASTER HISTORY: Y N (U)
 26. LAND USE: U 1 2 (3) 4-D 1 2 (3) 4
 27. FPM REC: 1 2 3 4 (5) 6 7

PART IV - FOR FEMA USE ONLY

28. AMOUNT ELIG \$
 29. ELIGIBLE Y N S V
 30. SPECIAL CONSIDERATIONS
 31. FLOODPLAIN REVIEW NO. [] [] [] [] [] [] [] [] [] []
 32. WORKSITE NO.
 33. INSURANCE COMMITMENT REQUIRED: Building: \$ Property: \$ Content: \$ Content: \$
 34. DURATION (Years): F: B: G: P: C: C:

35. COMMENTS/CHANGES

FIRST REVIEW (Signature) | DATE | SECOND REVIEW (Signature) | DATE

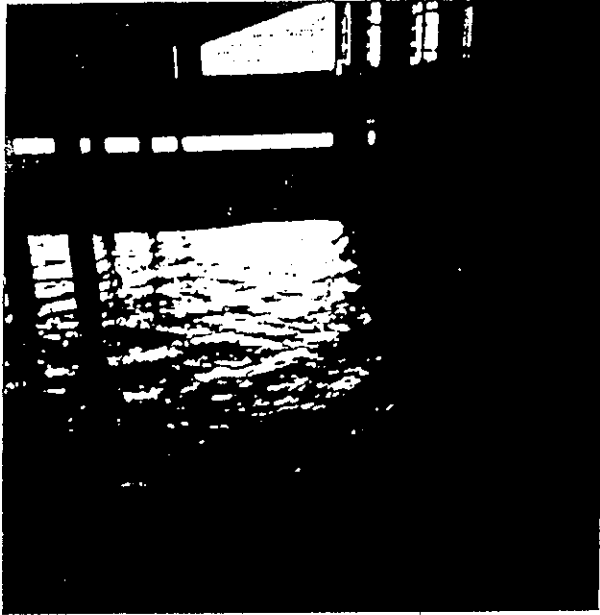


Photo No. 1

Item No. 1 AND 3

Description TYPICAL SPALLING OF
BEAMS. NOTE EXPOSED AND CORROD
REINFORCEMENT. TOTAL NUMBER
OF DETERIORATED BEAMS = 9.
SPALLS EXTEND TO ± 10 FEET A
THE BEAMS.
TOTAL SPALLING LENGTH = 9 x 1

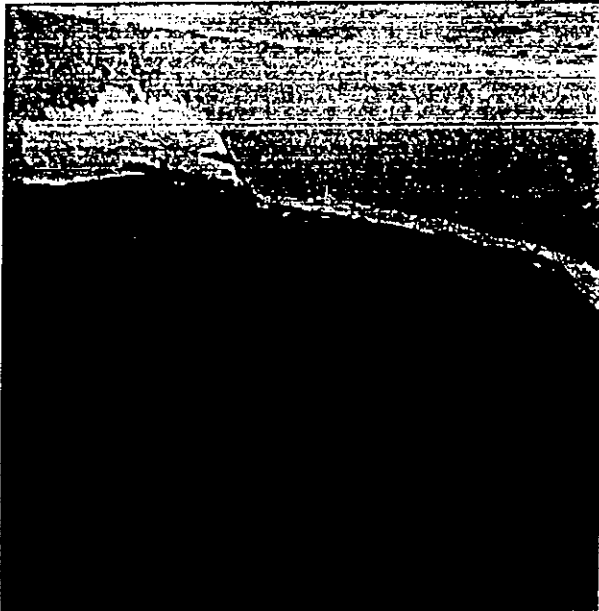


Photo No. 2

Item No. 1 AND 3

Description CLOSE-UP AT CONCRET
SPALLING OF GRADE BEAMS.



PILE/COLUMN
TYPICAL CONC. SPALLING
MARINA STADIUM

Photo No. 3

Item No. 5

Description CONCRETE SPALLING OF
PILES TYPICAL. TOTAL NUMBER
OF SPALLED PILES = 6. SPALLS
EXTEND 4' ALONG THE DETERIORATE
PILES.

TOTAL DETERIORATED PILE LENGTH
= 4 X 6 = 24 LF

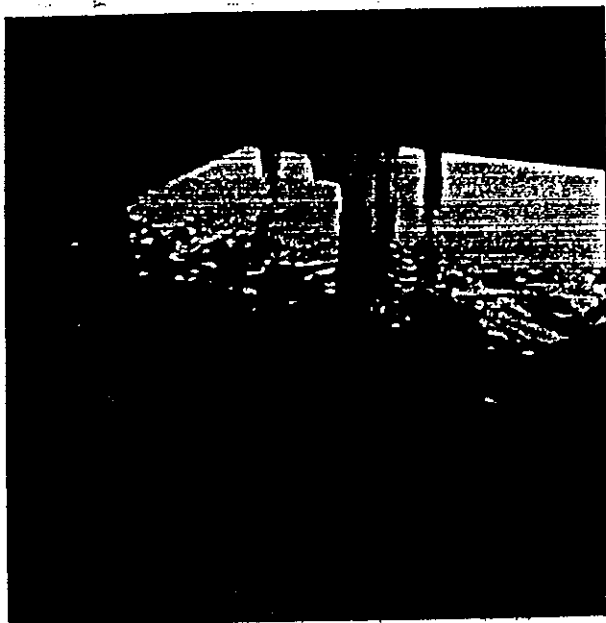


Photo No. 4

Item No. 5

Description TYPICAL PROPOSED
REPAIR OF PILES.

ATTACHMENT 2

TO DSR NO. 29220

APPLICANT CITY OF MIAMI

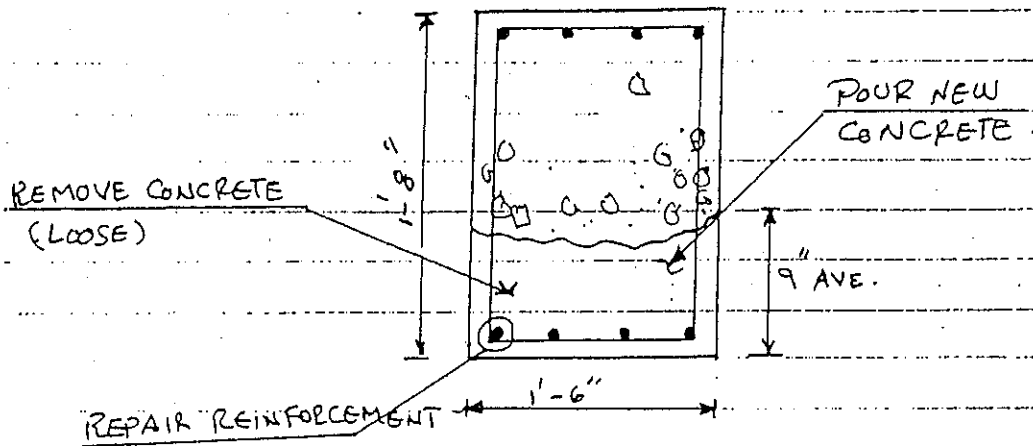
PA # 02545000

DSR # 29220 ATTACHMENT

Title SUBSTRUCTURE REHABILITATION, MARINE STADIUM Job No. _____

Subject _____ Sheet No. _____ of _____

FOR UNIT COST, SEE ATTACHMENT #1



GRADE BEAM TYPICAL REPAIR

ITEM 1. CONCRETE REMOVAL

BEAMS DETERIORATED = 9
 LENGTH OF DETERIORATION = ± 10'
 TOTAL LENGTH = 9 x 10' = 90'
 TOTAL CONC. REMOVAL = 90 x 0.75 x 1.5 = 101 SAY 110 CF

ITEM 2. REINFORCEMENT REHABILITATION

ASSUME 50% OF THE BARS ARE DETERIORATED

LF = $\frac{50}{100} \times 4 \times 90' = 180'$ 180 LF

ITEM 4. SURFACE SEALER

SURFACE AREA / BEAM = 1.5 + 2 x 0.75 = 3 SAY 3 SF

TOTAL = 4 x 90' = 360 LF SAY 360 LF

PSK 24220

FORMAL BID

ATA No. 4

MARINE STADIUM STRUCTURAL REPAIRS PHASE II - (ALTERNATE BID B)

Project Number: _____

Project Manager: KARL THOMPSON

Person who received the bids: KARL THOMPSON

Construction Estimate = \$ _____

CIP Number: _____

Date: _____/_____/____

Received at: CITY CLERK'S OFFICE

Time: 11:30 A.M.

SMITH HAMMOCK
LANDSCAPE INC.
28225 S.W. 172ND AVE
HOMESTEAD

CONSOLIDATED
TECHNIQUES, INC.
701 S.E. OKEECHOBEE
RD. HIALEAH

ALL CONSTRUCTION,
INC.
7390 S.W. 116 TERR.
MIAMI

MCM CORPORATION
1401 S.W. 1ST ST.
#205, MIAMI

BIDDER

CHECK \$10,000.00

B.B. VOUCHER

5% B.B.

H

YES

H

YES

YES

YES

YES

UNIT PRICE

TOTAL

UNIT PRICE

TOTAL

UNIT PRICE

TOTAL

UNIT PRICE

TOTAL

UNIT PRICE

TOTAL

NO BID

\$460.00

\$18,200.00

\$75.00

\$30,000.00

\$184,000.00

\$122.00

\$36,840.00

\$142.50

\$57,000.00

\$34.50

\$13,800.00

\$25.50

\$9,000.00

\$22.50

\$5.75

\$40,250.00

\$7.10

\$7,000.00

\$1.00

\$20,700.00

\$3,450.00

\$8,800.00

\$1,700.00

\$10,200.00

IRREGULARITIES LEGEND

- A - No Power-of-Attorney
- B - No Affidavit as to Capital & Surplus of Bonding Company
- C - Corrected Extensions
- D - Proposal Unsigned or Improperly Signed or no Corporate Seal
- E - Incomplete Extensions
- F - Non-responsive bid
- G - Improper Bid Bond
- H - Corrected Bid
- I - No First Source Hiring Compliance Statement
- J - No Minority Compliance Statement
- K - No Duplicate Bid Proposal

IT HAS BEEN DETERMINED BY THE DEPARTMENT OF PUBLIC WORKS THAT THE LOWEST RESPONSIBLE AND RESPONSIVE BID IS FROM _____ FOR THE TOTAL AMOUNT OF _____

If the above contractor is not the lowest bidder explain:

VOK 2960

FORMAL BID

ATJA. No. 5

MARINE STADIUM STRUCTURAL REPAIRS PHASE II - (ALTERNATE BID B)

Project Number: _____ CIP Number: _____
 Project Manager: KARL THOMPSON Date: / /
 Person who received the bids: KARL THOMPSON Received at: CITY CLERK'S OFFICE
 Construction Estimate = \$ Time: 11:30 A.M.

BIDDER: GUNITE CONSTRUCTION RENTALS, INC. ADDRESS: 1701 N.W. 2ND COURT MIAMI.
 BID BOND AMOUNT: 5% B.B.
 IRREGULARITIES: _____
 MINORITY OWNED: NO

SNAPP INDUSTRIES, INC. ADDRESS: 2902 N.W. 22 ST. MIAMI.
CHECK \$7,053.95
B.B. 5%

STRUCTURAL PRESEV. SYSTEMS ADDRESS: 4720 N.W. BOCA RATON BLVD. BOCA RATON
C. CHECK

AARYA CONSTRUCTION INC. ADDRESS: 960 ORIOLE AVE. MIAMI SPRINGS.

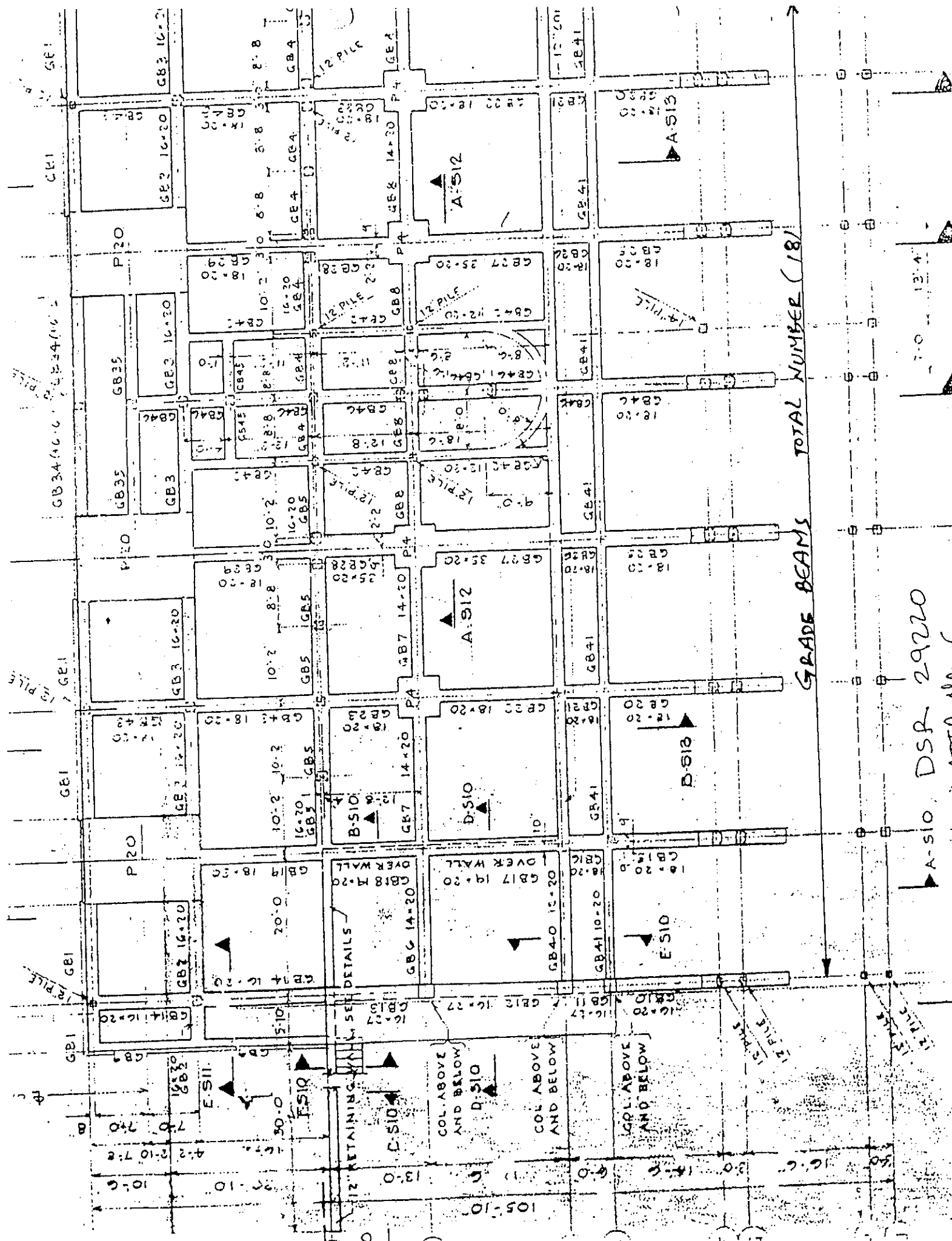
ITEM No	DESCRIPTION	GUNITE CONSTRUCTION RENTALS, INC.		STRUCTURAL PRESEV. SYSTEMS		SNAPP INDUSTRIES, INC.		AARYA CONSTRUCTION INC.	
		UNIT PRICE	TOTAL	UNIT PRICE	TOTAL	UNIT PRICE	TOTAL	UNIT PRICE	TOTAL
1	Removal of approx. 400 c.f. of damaged and deteriorated reinforced concrete.	\$45.00	\$18,000.00	\$50.00	\$20,000.00	\$60.00	\$24,000.00	\$57.00	\$22,800.00
2	400 c.f. of formed and poured concrete mortar	\$124.80	\$49,920.00	\$137.00	\$54,800.00	\$135.00	\$54,000.00	\$92.00	\$36,800.00
3	100 linear feet steel reinforcement	\$12.00	\$4,800.00	\$4.00	\$1,600.00	\$7.50	\$3,000.00	\$19.00	\$7,600.00
4	7,000 s.f. of surface coating	\$95	\$6,650.00	\$1.50	\$10,500.00	\$91	\$6,370.00	\$1.65	\$11,550.00
	For the repair of 6 concrete piles	\$1,200.00	\$7,200.00	\$925.00	\$5,550.00	\$450.00	\$2,700.00	\$1,825.00	\$10,950.00

IRREGULARITIES LEGEND
 A - No Power-of-Attorney
 B - No Affidavit as to Capital & Surplus of Bonding Company
 C - Corrected Extensions
 D - Proposal Unsigned or improperly Signed or no Corporate Seal
 E - Incomplete Extensions
 F - Non-responsive bid
 G - Improper Bid Bond
 H - Corrected Bid
 I - No First Source Hiring Compliance Statement
 J - No Minority Compliance Statement
 K - No Duplicate Bid Proposal

IT HAS BEEN DETERMINED BY THE DEPARTMENT OF PUBLIC WORKS THAT THE LOWEST RESPONSIBLE AND RESPONSIVE BID IS FROM _____ FOR THE TOTAL AMOUNT OF _____

If the above contractor is not the lowest bidder explain:

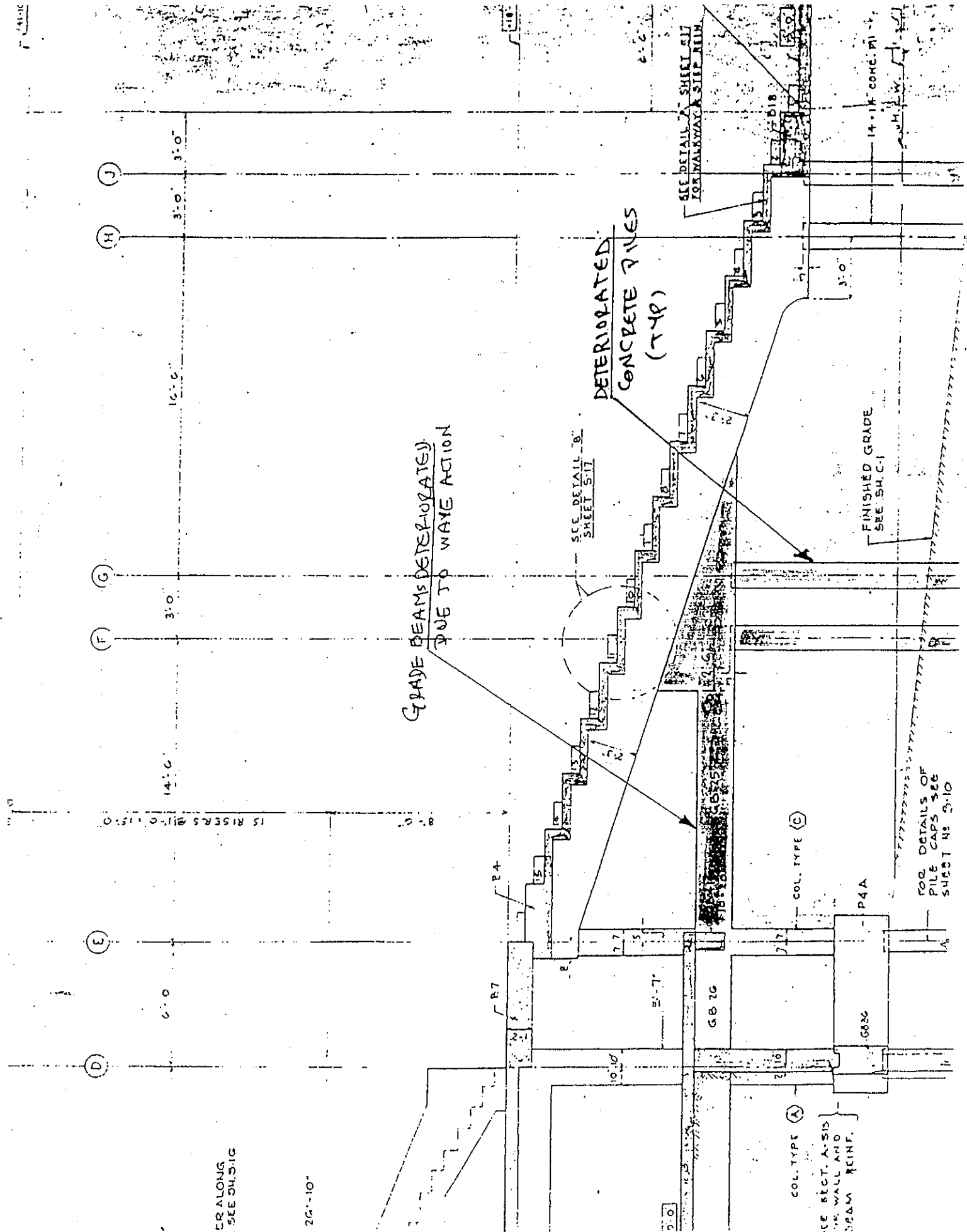
Prepared By: J Peret



GRADE BEAMS TOTAL NUMBER (18)

A-S10 DSR 2920

7'-0" 13'-4"



DSR 29220

DEPARTMENT OF PUBLIC WORKS

Damage Estimate

Structure: Marine Stadium

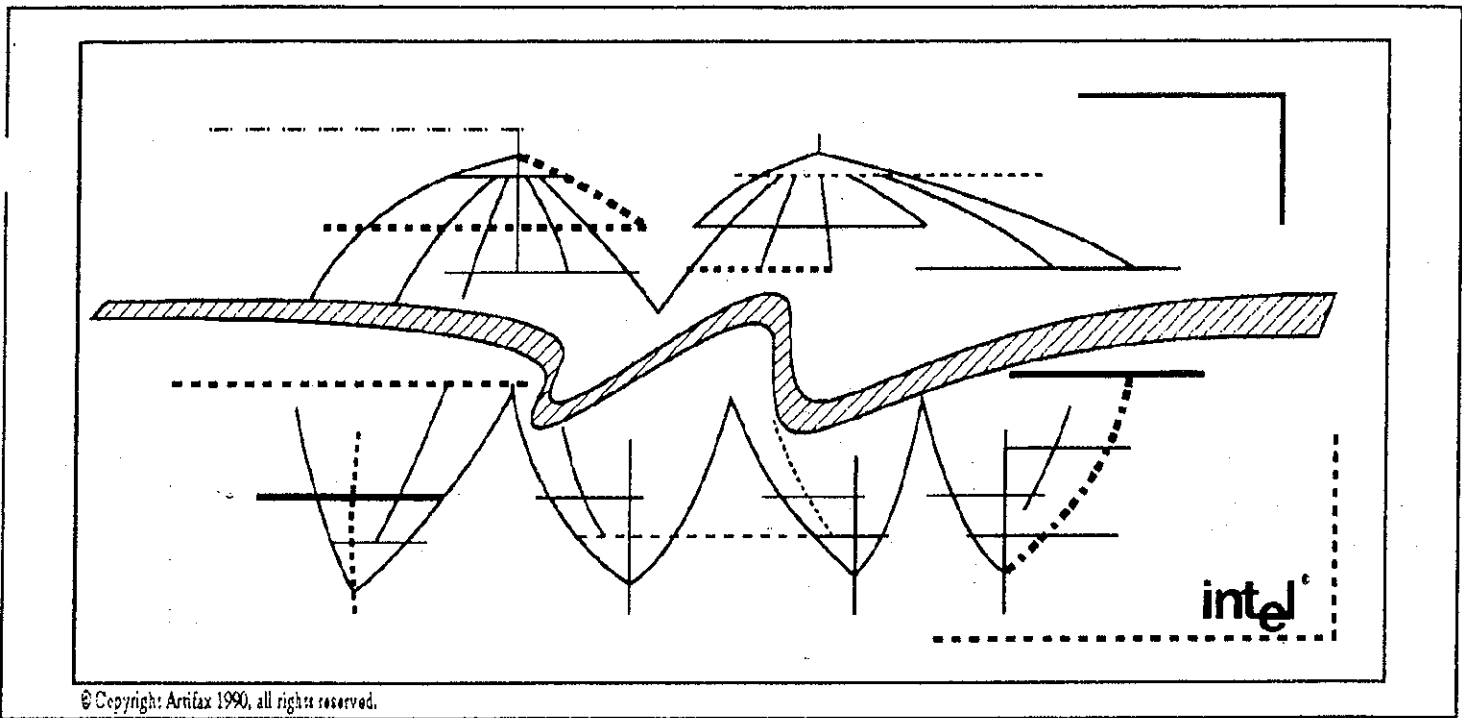
Location: 3601 Rickenbacker Csway

Scope of Work:

Furnish all labour, equipment and materials for the structural repair to damaged beams and columns as well as piles. Work shall include removal damaged concrete, sandblasting, reinforcement rehabilitation, application of bonding/corrosion agent, repair material and surface sealer/coating. Pile repair shall employ the use of pile jackets to be filled with epoxy grout mortar. (See attached Diagrams)

ITEM#	DESCRIPTION	UNIT OF MEASURE	QUANTITY	UNIT PRICE	COST
1	Repair of damaged beams and columns Removal of deteriorated concrete - \$60/cu. ft.; SikaTop 122 or equal (material only) - \$36/unit, yield = 0.4 cu.ft./unit; Arimatec 110 (material only) - \$140/unit, yield = 25 sq.ft./unit	cu. ft.	400	\$200.00	
2	Pile Jacketing of damaged piles	each	6	\$1,200.00	
3	Replacement of surface coating/sealer SikaTop 144 - \$106/5 gal. unit, yield = 100 sq.ft./gal Sikaguard 70 - \$142/5 gal unit, yield = 100sq.ft./gal	sq. ft.	7000	\$1.75	

material only



To: HURRICANE RECOVERY TEAM

Date: 10-14-93

From: Victoria LaGuette

Page 1 of 2

DEAR CHIEF ROLLASON

JUST WANTED YOU TO HAVE A COPY OF MY LETTER TO PAUL KELLY.

WHEN I CHECKED WITH OUR BOARD, IT WAS RECOMMENDED THAT

"ABSENCE" SHOULD BE SUBSTITUTED FOR "NEGLECT", AND

"REGULAR" SHOULD BE SUBSTITUTED FOR "NORMAL".

"SIMPSON GUMPERTZ & HEGER" IS A HIGHLY REPUTABLE AND VERY WELL RESPECTED CONSULTING ENGINEERING FIRM. WE WOULD NEVER ASK THEM TO DO ANYTHING UNPROFESSIONAL. (IT DID NOT EVEN OCCUR TO US TO CONTACT THEM AT ALL, UNTIL THAT MORNING BEFORE THE MEETING!)

WE APPRECIATE VERY MUCH YOUR DEPENDABLE PROFESSIONALISM, AND YOUR (ALWAYS) PROMPT RESPONSE TO OUR INQUIRIES.

MANY THANKS AND BEST WISHES

.v1.
662-5601

RUFUS NIMS
ARCHITECT
FOUNDATION

ESTABLISHED TO PROMOTE INNOVATIVE
DESIGN AND CONSTRUCTION OF
ENVIRONMENT RESPONSIVE ARCHITECTURE

POSTOFFICE BOX 248852
CORAL GABLES FL 33124

3 0 6 . 6 6 2 - 6 6 0 1

12 October 1993

FAX page 1 of 11

Paul Kelly PE
SIMPSON GUMPERTZ & HEGER INC.
297 Broadway
Arlington, MA - 02174
617.643-2000
FAX 617.643-2009

Dear Mr. Kelly

Thank you for your willingness to check, if it might be appropriate for SIMPSON GUMPERTZ to FAX us a letter, which very briefly outlines the main points of your Structural Engineering Survey Summary of MIAMI MARINE STADIUM.

In particular, did you find evidence of any

"extensive hurricane damage"?

"neglect of normal maintenance" of the structure?

We are sending you the following materials, just in case you may find something relevant.

Sorry to have contacted you so late about this meeting tonight.

I will call again, as agreed, after 1.30pm.

Many thanks for your understanding.

Best wishes

.vl.

Victoria LaGuette
Executive Director

c.c. J. Nyitray PE
M. C. Harry AIA

FOUNDING DIRECTOR
VICTORIA LAGUETTE

BOARD OF DIRECTORS
HERNANDO ACOSTA ARCHITECT
WILFREDO BORRERO ARCHITECT
R. DAVID BUTT
WILLIAM COX ARCHITECT
MILTON C. HARRY ARCHITECT
CHARLES HARRISON PAWLEY ARCHITECT
BRAD SCHIFFER ARCHITECT

VERY - MUCH - ALIVE
RUFUS NIMS ARCHITECT

JR Builders, Inc.

240 Collins Ave., #6D
Miami Beach, FL 33139

June 8, 1993

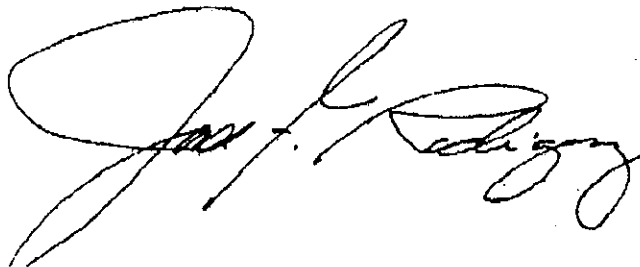
Mr. Paul Kelley
Simpson Gumpertz & Heger Inc.
297 Broadway
Arlington, MA. 02174-5310

Re: Request for Quotation
Demolition Services
Marine Stadium, Key Biscayne

JR Builders, Inc. hereby proposes to furnish all permits, materials, labor, supervision, and transportation necessary in demolishing the above referenced project. Demolition as specified to top of the existing piling caps. This quotation does not include an asbestos survey, removal of any asbestos containing material, or asbestos abatement supervision.

Contract Sum:
Four Hundred Sixty Nine Thousand Dollars.....\$469,000.00

From the time Contractor is presented with " Notice to Proceed with Contract Work" Contractor will guarantee completion of work within one hundred twenty (120) calendar days thereafter. This price is good for thirty (30) calendar days.



Jose F. Rodriguez, President
JR Builders, Inc.
JFR:vm

cc: Mr. Grant Sheehan